Evolutionary model for glacial lake-outburst fans at the ice-sheet front: development of meltwater outlets and origins of bedforms

Piotr Weckwerth[1], Edyta Kalińska[1], Wojciech Wysota[1], Arkadiusz Krawiec[1], Helena Alexanderson[2, 3], Marek Chabowski[1]

1 – Nicolaus Copernicus University in Toruń, Poland

2 – Lund University, Sweden

3 – University of Tromsø, Norway

Corresponding author: Piotr Weckwerth, email: pweck@umk.pl

Abstract

Large-scale landforms originated from jökulhlaups or glacial lake-outburst floods (GLOFs), and their small-scale components help in recognising the sedimentary environment of the flood. The GLOF fans that developed along the Pleistocene ice-sheet margin have not been investigated in detail, and north-eastern Poland, with its Megaflood Landform System and Bachanowo and Szeszupka fans, seems ideal for landform and sedimentary studies. This paper provides (1) an important opportunity to recognise the origins of glacier lake-outburst flood outlets and their evolution during two GLOFs and (2) a model of the origin of ice-marginal fans considering changes in sedimentary environment reflecting flood stages. During the first GLOF (GLOF1), the rising stage of meltwater burst triggered the formation of a supraglacial outlet and the development of the Szeszupka outburst fan. During the pulsed peak discharge, subglacial multi-channelised meltwater outburst caused the formation of the Bachanowo Gate, which was finally transformed at the flood waning stage. Such processes were associated with

the widening of the floodwater subglacial routeway, when floodwater outlets rapidly spread across the glacier snout. In contrast, GLOF2 was responsible only for the Szeszupka fan erosion and development of outburst terraces. The small-scale bedforms continuum, recognised on the outburst fan surface, is associated with the development of streamlined erosional residuals, scours and their trains during the rising stage and peak discharge, while the waning stage and very end of flood conditions were favourable to the formation of pendant bars, distributive channels with erosional bars and chute bars, regardless of the feeding systems of the outburst fans.

The fan deposits were OSL-dated and revealed either, likely, overly old ages or an age of 13.2±0.9 ka. The latter age would imply the 'normal' meltwater outflow having a correlation with the events in the region. Nevertheless, this age might be considered a minimum age of the flood.

Keywords: glacial lake-outburst flood, outburst fan, meltwater outlet, glacial curvilineation, Poland, Weichselian glaciation

1. Introduction

Landforms and sediments associated with volcanically-generated jökulhlaups or glacial lake-outburst floods (GLOFs) from ice-dammed lakes have been described widely, and large-scale features indicative of these GLOFs comprise both erosional landforms (e.g., residual ridges and erosional bars) and depositional landforms (e.g., jökulhlaup fans, expansion bars, pendant bars, dunes) scaled to the flood channel width and depth (e.g., Baker, 1973; Lord and Kehew, 1987; O'Connor, 1993; Maizels, 1997; Marren et al., 2002; Kozlowski et al., 2005; Carrivick and Rushmer, 2006; Russel et al., 2006; Carling et al., 2009a, 2010; Marren and Shuh, 2009; Meinsen et al., 2011; Lang et al., 2019; Weckwerth et al., 2019; Wells et al., 2022). Small-scale bedforms are component elements of the main GLOF-related features. As such, identifying the processes and factors controlling the development of these landforms plays a crucial role in recognising the sedimentary environments of GLOFs, which are highly variable (Marren and Shuh, 2009; Carling, 2013; Wells et al., 2022).

GLOF-related small-scale bedforms can form continua in terms of their spatial (downstream) and temporal changes in sedimentary environments (i.e., variations in sediment flux, flood magnitude and its rising or falling stages). The first (spatial) continuum relates to downstream variations in the morphology of the large-scale GLOF-related landforms, while the temporal continuum is displayed in their sedimentary successions (e.g., Russel and Knudsen, 1999, 2002b; Carling, 2013; Wells et al., 2022). As many studies indicate, the most common bedforms originating from supercritical flow that are recorded in the sedimentary successions of the GLOFs are gravel bedload sheets, cyclic-steps, chutes-and-pools and antidunes developed in confined or semi-confined settings and forming large bedforms (e.g., Russell et al., 2006; Rushmer, 2006; Duller et al., 2008; Russel, 2009; Marren and Shuh, 2009; Winsemann et al., 2011, 2016, 2018; Girard et al., 2012; Carling, 2013; Lang and Winsemann, 2013; Lang et al., 2021; Weckwerth et al., 2022). Nevertheless, bedforms and sediments typical of Froude-supercritical flow may originate at the very end of the flood (Maizels, 1993; Russell and Marren, 1999; Smith, 1993; Shaw et al., 1999; Marren, 2002; Carling et al., 2009b, 2013; Lang and Winsemann, 2013; Winsemann et al., 2016).

A wide range of different bedforms, mostly related to Froude-supercritical flow, has been interpreted from sedimentary successions of GLOF-related subaqueous ice-marginal fans and deltas (Russel et al., 2006; Winsemann et al., 2009, 2011, 2016, 2018; Lang and Winsemann, 2013; Lang et al., 2021; Weckwerth et al., 2022) or developed in subaerial settings interpreted as a result of catastrophic meltwater outflow (e.g., Zieliński and van Loon, 2000; Krzyszkowski, 2002; Krzyszkowski and Zieliński, 2002; Kjær et al., 2004). As pointed out in many studies, the morphology and processes forming ice-marginal fans and deltas originating from GLOFs are closely associated with the floodwater outlet morphology, flow confinement, characteristics of peak flood discharges and waning flow conditions, rate of sediment flux, and backwater level changes (e.g., Russell and Knudsen, 1990, 2002b; Blair 2001, 2002; Gomez et al., 2002; Benn et al., 2006; Russel et al., 2006, 2007; Russell, 2009; Weckwerth et al., 2019; Harrison et al., 2022, 2023). In many cases, these circumstances have not been considered in investigations into the evolution of ice-marginal fans along the margin of the Pleistocene ice sheets. Although the morphology of proglacial areas has been analysed in terms of contemporary development of ice-contact fans and their sedimentary successions (e.g., Russell and Knudsen, 1990, 2002b; Gomez et al., 2000, 2002; Russel et al., 2006; Weckwerth et al., 2019, 2021), little attention has been paid to downstream changes in bedform types and their sedimentology for outburst fans developed under special conditions (i.e., in laterally confined, subaerial settings of the proximal reaches of spillways and those that originated from the drainage of meltwater stored in non-volcanic subglacial lakes during the last glaciation) (e.g., Kehew and Teller, 1994; Clayton et al., 1999; Cutler et al., 2002; Kozlowski et al., 2005; Jørgensen and Sandersen, 2006; Weckwerth et al., 2019, 2022; Wells et al., 2022; Weckwerth and Wysota, 2024).

Considering the aforementioned research problems and gaps, this study examines geomorphological and sedimentological records of GLOFs that relate to the formation of subaerial outburst fans; it also provides an opportunity to improve existing models of evolution of the fans under the specific conditions of laterally confined settings and in association with the formation of GLOF outlets during meltwater release from non-volcanic subglacial lakes at the end of the last glaciation. In these contexts, our objectives here are to (1) describe, discuss and interpret the sedimentary environments and geomorphic features produced by GLOFs at the submarginal position and at the front of two types of floodwater outlets; (2) recognise bedform types, their spatial and temporal continuum and factors influencing their development, (3) present a qualitative model for the evolution of floodwater outlets and associated subaerial outburst fans and their bedforms considering changes in the englacial feeding system, and (4) attempt a chronological frame of the GLOF.

2. Geomorphological setting

The study area is located in north-eastern Poland and partly covers the Western and Eastern Suwałki Lakelands, which are composed mostly of glacial deposits forming a moraine upland (Fig. 1B). Its morphology is characterised by ice-marginal and dead-ice features related to the recession of the Scandinavian Ice Sheet at the decline of the Weichselian Glaciation (MIS 2) (Kondracki and Pietkiewicz, 1967; Ber, 1974, 1982, 2000). The moraine upland is dissected by large tunnel valleys that developed in a subglacial setting, namely the Szeszupa Tunnel Valley, the Jeleniewo Tunnel Valley, the Great Szelment Lake Tunnel Valley and the Hańcza Lake Tunnel Valley (Fig. 1). With the exception of the Hańcza Lake Tunnel Valley, these all evolved during glacial lake-outburst floods and represent first-order landforms of such origin (Weckwerth et al., 2019; Wysota and Weckwerth, 2024). The second-order subglacial and flood-related features are glacial curvilineations (GCLs), composing clusters of parallel ridges separated by troughs of different lengths, widths and heights.

The Western and Eastern Suwałki Lakelands are intersected by the Augustów Plain (the Suwałki-Augustów sandur) (Fig. 1A, B). This outwash plain (sandur) was formed by proglacial meltwater activity during the Late Weichselian (Kondracki and Pietkiewicz, 1967; Ber, 1974; Bogacki, 1976, 1980; Zieliński, 1989, 1993; Weckwerth et al., 2019). Its surface drops from north to south, from ~190–170 m a.s.l. near Suwałki to ~130–140 m a.s.l. near Augustów, comprising a system of four main topographic (outwash) levels (1–4) (Fig. 1).

It is thought that the northern part of the Suwałki-Augustów sandur developed during the ice-sheet retreat of the Pomeranian phase of the Weichselian glaciation (Bogacki, 1976; Zieliński, 1989, 1993; Zieliński and Van Loon, 2003) and includes two separate tracks of meltwaters, namely the Western and Eastern Spillways (Fig. 1). These formed as a result of a glacial lake-outburst megaflood (Weckwerth et al., 2019) and represent the first-order proglacial landforms in the Proglacial Megaflood Landform System (as a part of the Megaflood Landform System) that merge around Suwałki town (Figs 1A–C). The megaflood-related second-order landforms cover scabland-like topography, subaerial outwash (outburst) fans, obstacle marks, megadunes and clusters of kettle holes (Weckwerth et al., 2019) (Figs 1A–E and 2).

Two subaerial outburst fans, i.e. the Bachanowo and Szeszupka Fans, developed in the proximal reach of the Western Spillway, which is 12.1 km long and up to 4.5 km wide and comprises three outwash levels (Figs 1 and 2). During the GLOFs, this spillway existed as an ice-walled canyon fed by floodwaters flowing from the Bachanowo and Szeszupka Gates (ice portals) (Fig. 1A–C). Each of the two fans started to form at the front of these floodwater outlets and at the mouth of the Szeszupa Tunnel Valley (the Bachanowo and Szeszupka outburst fans) (Figs 1 and 2).

3. Methods

3.1. Geomorphological mapping and morphometry analysis

The landforms originating from GLOFs in the study area were mapped on the base of DEMs with pixel size 1×1 m (generated from LiDAR data). The geomorphological mapping of terrain features was conducted after superimposing the DEMs and hillshade images (relief map with solar azimuths of 315° and solar angle of 45°), which allowed the detection error to be minimised (Schillaci et al., 2015). After the landform locations were mapped, their morphometric parameters were measured as length (L), width (W), depth (D), height (H) and orientation (A – azimuth of the strike in degrees) using GIS tools (ArcGIS 10.8.1).

3.2. Lithofacies analysis

Genetic classification of the sediments and the types of lithofacies were performed for six key sites on the Bachanowo and Szeszupka outburst fans. Due to the lack of gravel and sand pits, it was necessary to cut 4-5-m deep and a 4-5-m wide trenches, using an excavator. Thus, the description and interpretation of sedimentary structures were based on rather small excavations, and to avoid misinterpretation, lithofacies were investigated on all four of the trenches walls, which were perpendicular to each other. The sedimentary lithofacies at the key sites were identified using the terminology and lithofacial coding after Miall (1978, 2006), Krüger and Kjær (1999), Cofaigh et al. (2011) and Lang et al. (2021) (Table 1). As a result, sedimentary facies associations (units) were defined and the depositional environments and bedform origins were interpreted taking into account the textural and structural properties of the sediment (Table 1) (cf. Bridge, 1993; Lang et al., 2021).

3.3. Grain-size distribution

The grain-size distributions of sediments were assessed by sieving at 1-φ intervals for sands and gravels, while the silt and mud fractions were measured at 0.25-φ intervals using a laser particle-size analyser (Analysette 22). The results enable the determination of the textural types of sediments according to the scale proposed by Wentworth (1922), and sediment classes and names were defined by the percentage of gravel and the ratio of sand to silt and clay. The statistical parameters for the grain-size distributions were calculated using the geometric method of moments, and are median grain diameter (d_{50}), sorting (σ), skewness (Sk) and kurtosis (Kg).

3.4. Geophysical research

Ground-penetrating radar (GPR) was used to investigate geological structure and sediment variability in detail (Jol, 2008) along profiles that intersected the Bachanowo outburst fan perpendicular to the direction of floodwater outflow. A LEICA DS2000 with dual-head sensor integrating ultra-wide band antennae (250 MHz and 700 MHz) was used, and ReflexW was used software for processing and interpretation.

3.5. Sediment age determination

Wherever available, ~25-cm thick sandy beds were sampled for optically-stimulated luminescence (OSL) dating by hammering four opaque plastic tubes into the freshly cleaned walls (Figs 8A and 11A). Samples were further prepared in the Lund Luminescence Laboratory, Sweden. The inner part of the sediment was wet-sieved, and the 180–250-µm fraction was used for chemical treatment (10% HCl, 10% H_2O_2 and density separation at 2.62 g/cm^3). After separation, the quartz extract was treated with 40% HF, followed by 10% HCl to remove fluorides.

Small 2-mm aliquots of quartz extracts were analysed in a Risø TL/OSL reader model DA-20 (Bøtter-Jensen et al., 2010) with OSL stimulation by blue light sources (470±30 nm) and detection through 7 mm of U340 glass filter. The 180–250 µm quartz fraction was measured with post-IR blue stimulation, because of the high feldspar contamination. The standard dose recovery test was passed with a value of 0.95±0.04 (n=12). To obtain the equivalent dose (D_e; dose), between 23 and 28 aliquots were accepted.

Historical water content was set as 11%±5%. High-resolution gamma spectrometry was used to determine the sediment dose rate (Murray et al., 1987) at the Nordic Laboratory for Luminescence Dating, Aarhus University, Denmark. Later, based on the DRAC online calculator (Durcan et al., 2015), the environmental dose was calculated.

4. Results

The Bachanowo and Szeszupka outburst fans (BOF and SOF, respectively) developed at the mouth of the Szeszupa Tunnel Valley (Figs 1 and 2), and thus the origin of landforms in subglacial flood routeway at submarginal position was analysed because it plays a crucial role in the recognition of evolutionary stages for both outburst fans. Moreover, these fans are characterised by proximal zones located along ice-marginal sedimentary escarpments (Figs 1C–E and 2) and the intermediate zone located between the BOF fan apex and subglacial flood routeway. In addition, the BOF and SOF are incised into pre-existing moraine uplands and thus are confined by slopes of heights up to 16 m (Figs 1 and 2). The fans are located close to each other, and their lower reaches form one morphological level, which continues southwards to form the highest (main) outburst terrace (T1) in the Western Spillway, which corresponds to outwash level 2 of the Suwałki-Augustów sandur (Figs 1B, D and 2C, D).

4.1. Morphology and origin of landforms in subglacial flood routeway and at submarginal position

The Szeszupa Tunnel Valley, as the major floodwater routeway, consists of a few widenings and erosional levels of different heights, the southernmost of which developed near to the BOF and SOF (Figs 1 and 2).

4.1.1. Subglacial landforms near the Bachanowo outburst fan

Subglacial landforms at the contact of the BOF cover two morphological levels, the heights of which increase from 210 to 248 m a.s.l. towards the former ice-sheet margin, where the floodwater outflow (the Bachanowo Gate) occurred (Figs 1–3 and 4A, B). The first type of subglacial features is represented here by a cluster of arcuate ridges, which are parallel to the estimated and local subglacial flow direction and separated by troughs of depths up to 30 m (Figs 1–3). The southern ends of these ridges pass to the BOF or drop towards the bottom of the Szeszupa Tunnel Valley. Individual ridges are up to 100–400 m wide and up to 3 km long.

These landforms have surfaces occupied by boulder pavements occurring at altitudes of 210–260 m a.s.l., being similar to the height of the neighbouring moraine upland (Figs 1D and 2A, C). In addition, parallel ridges near Łopuchowo have uneven crest lines that undulate by up to 20 m and are also capped by narrow, superimposed eskers (Figs 1E and 2C). The morphological characteristics of the arcuate and parallel ridges near Łopuchowo allow them to be interpreted as glacial curvilineations of exceptionally large size formed as erosional remnants of the antecedent substratum having been carved by flows of subglacial meltwaters (Figs 2C and 3A) (Lesemann et al., 2010, 2014; Wysota et al., 2020; Adamczyk et al., 2022; Hermanowski and Piotrowski, 2023).

The second type of subglacial landforms lying upflow of the Bachanowo Gate is represented by a set of semi-parallel and poorly-developed ridges of heights up to 6 m and widths up to 120 m, which reach 400 m in length and occur on the higher erosional level (Figs 2C and 3A). These ridges are interpreted as initial GCLs, which constitute a morphological continuum with the well-developed GCLs, considering that their crest lines have the same orientation and the heights of their top surfaces are similar; however, the troughs separating them decrease in depth towards the ice-sheet margin (Figs 2C, 3A and 4B). According to these characteristics, initial GCLs were shaped under conditions of meltwater pressure near the ice-sheet margin that was lower than for the larger and well-developed GCLs near Łopuchowo (Lesemann et al., 2010, 2014; Adamczyk et al., 2022).

4.1.2. Subglacial landforms near the Szeszupka outburst fan

The bottom of the Szeszupa Tunnel Valley at the contact with the Szeszupka outburst fan rises by 60 m over a distance of 2.5 km (from 170 to 230 m a.s.l.; Fig. 3B). Its steeper part occurs between the Wodziłki sub-basin and the bottom of the Szeszupa Tunnel Valley, where the adverse (up-ice dipping) surface descends to the north at an angle of 3.22°, which was probably favourable for glaciohydraulic supercooling (see Discussion). In addition, the bottom of the

Szeszupa Tunnel Valley is characterised by the occurrence of dead-ice topography in its lowermost part and a swarm of GCLs in the Wodziłki sub-basin (Figs 2B, D and 3B). The hummocky topography is dominated by isolated or grouped kames of heights up to 20 m separated by kettle holes of different shapes, while the swarm of GCLs comprises ten individual GCLs that are 400–890 m long and 30–75 m wide, lying between 196 and 218 m a.s.l. (Figs 2B, D and 3B). Their crests drop northwards to the bottom of the Szeszupa Tunnel Valley, while their arched south-western reaches are parallel to the SOF edge and end at the contact with the narrow proglacial valley incised into the outburst terrace T3 in the Western Spillway (Figs 1 and 2). Considering these, the GCLs in the Wodziłki sub-basin were formed by the erosion of pressurised subglacial meltwater flows (e.g., Lesemann et al., 2014; Adamczyk et al., 2022; Hermanowski and Piotrowski, 2023), which were not associated with the SOF formation.

4.1.3. Submarginal intermediate zone

4.1.3.1. Morphology

The intermediate zone (ITZ) was identified between the BOF apex and the swarm of the initial GCLs in the Szeszupa Tunnel Valley (Figs 2B, C; 3A and 4B). This zone is attributed to the highest morphological level in the southern margin of the Szeszupa Tunnel Valley and continues over a distance of 250–300 m to the BOF head, having an adverse subglacial bedslope that dips northward (up-ice) at 1.8° (Fig. 3A). Moreover, the morphology of the ITZ is characterized by a set of 1–2.5-m-high ridges interpreted also as initial GCLs up to 220 m long and 80 m wide, which fork to the south-west, i.e. towards the former floodwater outlet (Figs 2C, 3A, 4B and 5A).

4.1.3.2. Sedimentary succession

Facies description

The sediments of the ITZ were recognised at the Bachanowo 1 site (B1) located between ridges of initial GCLs (Figs 2C, 3A; 4A, B, 5A and Supplementary 1). Here, three sedimentary units U1–U3 were distinguished (Fig. 6). Unit U1 consists of horizontally laminated fine-grained sands and silts (Fig. 6). Lying above U1 are 3.7-m-thick sediments that form units U2 and U3. Unit U2 is represented by two sets of facies GBm, GRsc and GPsc (Fig. 6C, D). The lower position in each set is usually occupied by massive gravels and boulders with sandy matrix (GBm) of a thickness up to 0.8 m. These sediments are capped by sigmoidally cross-stratified granules and pebbles with admixture of sands (GRsc(GPsc)) each of up to 1.4 m thick (Fig. 6C, D). In the lower set, these deposits are better sorted and coarser than those in the upper set, and also exhibit openwork texture (Fig. 6C, D). Moreover, facies GRsc and GPsc have laminae that dip upstream and are concave-up across the palaeoflow, containing sandy rip-up clasts of lengths up to 1.1 m and thicknesses up to 0.45 m (Fig. 6C).

The uppermost sedimentary unit U3 in the Bachanowo 1 site is represented by deformed silts, sands of different fractions and large-scale clasts of diamicton (till), all affected by two systems of deformations (Fig. 6D–F). The first deformation system is bounded by two major, curved slip surfaces (normal faults) (mss1 and mss2 in Fig. 6A, C, D, F) and includes two diamicton (till) clasts, between which a diapir-like structure exists (ds in Fig. 4A, F). Its lower part is bounded by mss2, above which there occur rip-up clasts and sandy and gravelly boudins deformed by shear folds and microfaults (Fig. 6F). The upper part of the diapir-like structure consists of stratified or massive fine-grained sands and silts with patches of gravels. A set of small-scale folds and series of conjugate microfaults wrap around the large-scale till clasts (Fig. 6E).

The second system of deformations within unit U3 was identified southward of the mss1 in profile 2 and in the upper part of profile 3 (Fig. 6D). The deformed sediments form a narrow horst here (hs in Fig. 6D) that is bordered by normal faults lying at the contact with a narrow gravity-induced depression (gravifossum; Gruszka and van Loon, 2011) (gf in Fig. 6D).

Facies interpretation

The sedimentary succession in the Bachanowo 1 site documents the development of the ITZ, which was associated with floodwater release from the Szeszupka Tunnel Valley at the Bachanowo Gate (Figs 2 and 4A, B). Unit U1 is interpreted as a substratum of GLOF deposits that comprises sedimentary units U2 and U3 (Fig. 6). Two evolutionary stages and geomorphic processes in the ITZ refer to the GLOF sedimentary succession of these two units. At the beginning of the first stage (unit U2 deposition), the ice-sheet bed (unit U1) was scoured at the submarginal position and covered by lag deposits during the subglacial flood. Afterwards, the deposition of two sets of lithofacies associations GBm, GRsc/PGsc developed, and may indicate (1) rhythmic floodwater outflow, (2) two flood peaks, and/or (3) rapid temporal and spatial switching of depositional and erosional processes (Russell et al., 2001). The openwork texture suggests the intensive outwashing of fine fraction during initial peak-flow energy (Carling, 1990; Shaw and Gorrell, 1991; Weckwerth et al., 2022), through a combination of traction, buoyancy, and dispersive pressure (Pierson and Scott, 1985). The existence of rip-up clasts within unit U2 confirms rapid cut-and-fill processes, during which rip-up clasts in a non-frozen state can be deposited (Ito et al., 2014; Lang et al., 2017a). The ice-sheet bed disruption by floodwater and short-distance redeposition of large amounts of sediment occurred under condition of intense suspension fall-out. Regardless, it cannot be ruled out that floodwaters eroded permafrozen glaciogenic sediments and ice-sheet substratum to provide frozen rip-up clasts (Are 1983; Russell and Knudsen, 1990, 1999, 2002b; Roberts et al., 2001; Russell et al., 2001, 2005, 2006; Randriamazaoro et al. 2007; Weckwerth and Pisarska-Jamroży, 2014; Sobota et al., 2016, 2018).

The third, post-flood stage in the ITZ evolution, unit U3, reveals firstly meltwater outflow and the deposition of sands and gravels at the contact with ice blocks and secondly, subsequent accumulation of fine sediments in small ice-marginal lakes. The gravitational instability of these sediments, as an effect of degradation of ice walls and buried ice blocks (ice fractured during meltwater burst), triggered the development of a variety of soft-sediment deformation. Deformation processes (slumping and subsidence due to ice-blocks melting) caused two deformation systems to form in the ITZ, that are divided by a horst structure. The first system represents final, large-scale ice-marginal deformation associated with plastically upward movement of the glaciofluvial and limnoglacial post-flood sediments, finally forming a diapir-like structure due to lateral pressure exerted by the weight of the slumped till clasts and triggered by the removal of supporting ice blocks or ice walls (Roberts et al., 2000a, 2001; Russel et al., 2001; Blauvelt et al., 2020). The second deformation system is associated with a near-simultaneous gravifossum development due to the melting of ice-blocks buried by the outwash sediments (compare Gruszka and van Loon, 2011).

4.2. Outburst fans

4.2.1. Outburst fan morphology

The Bachanowo and Szeszupka outburst fans have lengths of 3.2 km and 1.2 km, respectively, while their maximum width is 1.2 for the BOF and 1.3 for the SOF (Fig. 3). Their surfaces have gradients of 0.0079 and 0.0005, respectively. The longitudinal profile of the BOF surface reveals upper (proximal) and lower (distal) zones (Fig. 3A). The proximal zone is characterised by a concave longitudinal profile, a length of 1600 m and a width of up to 1400 m. By contrast, the BOF distal zone is 1500 m long and 1120 m wide and has an almost uniform surface slope. The SOF is up to 1100 m wide and 1200 m long and has a uniform surface slope similar to the distal zone of BOF (Figs 2B and 3B). Additionally, the SOF surface is characterised by a reduction in lateral extension of its southern and south-western parts due to meltwater erosion forming the outburst terraces T2 and T3, and the lack of a proximal zone (similarly to the BOF) (Figs 2 and 3).

The morphology of both the BOF and the SOF displays a system of narrow and downstream elongated ridges. Their lengths (L) vary between 70 m and 687 m (average 254 m; n=18) for the BOF and 90–473 m (average 240 m; n=16) for the SOF, while widths are in the range 23–61 m (average 42 m) and 23–72 m (average 43 m), respectively. Considering these, the L/W ratio for the BOF ranged between 2.5 and 16.7 (average 5.8) and 3.2–10.8 (average 5.5) for the SOF. These ridges are separated by oval enclosed depressions (scours), which are up to 85 m long and up to 2.5 m deep and form scour trains in places. Elongated ridges also are separated by a network system of channels, mostly of braided pattern (Figs 2A, B, 4 and 5A–C). These channels and ridges merge upstream in the BOF apex (near the Bachanowo Gate; Figs 2A, C and 4A, B). Moreover, elongated ridges in the outburst fan distal part are further apart than those in its proximal zone (Figs 2A, B and 5).

Variable outburst fan morphology is typical of the slightly elevated areas that occur downstream of elongated ridges or at the mouth of scoured channels, which two features are interpreted as small-scale pendant and chute bars, respectively (Fig. 5C, F).

4.2.2. Sedimentary successions and bedform origins

Sedimentary successions of elongated ridges, bars and scours were recognised in five key sites (trenches B2–B4 and S1–2) and along two GPR profiles perpendicular to the palaeoflow direction (Figs 2, 4 and 7–11).

4.2.2.1. Downstream-elongated ridges

Facies description

The sedimentary succession of the elongated ridge in the proximal reach of the BOF was recognized in the Bachanowo 2 site (trench B2; Fig. 4). Here, massive, matrix-supported and clast-poor diamicton (Dm(m_1)) is capped by a 0.8-m-thick layer of sandy and massive diamicton (DSm(m_1)(d)) with deformed sandy clasts and sheared sand inclusions along the shear plane (reverse fault) dipping northward (Fig. 4D). The upper part of the sedimentary succession is of stratified and deformed sandy diamicton (DSs(m_1)) of a thickness up to 0.6 m and massive sands with admixture of gravels (SGm).

The GPR data reveal that the elongated ridges in the BOF proximal zone represent one dominant and two secondary reflection types (radar facies RF1–3; Fig. 7A). The dominant radar facies (RF1) are of very low-amplitude signal with sparse, chaotic and incoherent reflections. This facies (within the extent of elongated ridges) is interbedded by the secondary one, which is characterised by low amplitude, planar or wavy reflections (RF2) and capped by the radar facies with continuous and planar reflections (RF3; Fig. 7A).

In the distal zone of the BOF, the radar facies architecture of elongated ridges is variable, and their complex pattern is characterised by a system of alternating radar facies that dip in opposite directions, perpendicular to the palaeoflow, i.e. westwards and eastwards (Fig. 7B). Here, the basal radar facies (RF1) lies below those composing the flanks of two channel infills, between which elongated ridges developed. These radar facies are characterised by a strong, continuous and finely dense undulated reflection (RF4), very-high-amplitude, wavy and continuous reflections (RF5), low amplitude and locally noisy reflections (RF6) and low and moderate, continuous reflections (RF7) (Fig. 7B).

Facies interpretation

The sedimentary successions of the downstream-elongated ridges relate to two different depositional environments. The first is associated with the subglacial till deposition in the Bachanowo 2 site and subsequent till deformation as a result of compression in a subglacial setting during ice-sheet advance from the north and/or in the ice-marginal (proglacial) environment (Hart and Boulton, 1991; van der Wateren, 1999; Evans and Thomson, 2010). During the second phase, stratified diamicton and massive sands and gravels were deposited along the ice-sheet margin throughout its recession, as the ice-marginal fan surface was transformed by debris flows (Krzyszkowski, 2002; Krzyszkowski and Zieliński, 2002).

The dominant radar facies (RF1) composing the streamlined residual ridge in the Bachanowo 2 site is interpreted as massive and clay-rich sediments attenuating the radar signal, which infers the presence of massive diamicton (glacial till). The RF2 represents a layer of deformed sandy clasts and interbedded till. The RF3 corresponds to massive sands and gravels capping the surface of the elongated ridge (Figs 4D and 7A). Regardless of the origin of sediments in the Bachanowo 2 site, the interpreted depositional processes took place before the GLOF in an ice-marginal setting near to the Bachanowo Gate. Such an interpretation indicates that the elongated ridges in the proximal zone of the BOF are erosional remnants and fluvially-shaped, i.e. streamlined residual hummocks (*sensu* Baker (1978) and Maizels (1997); rh in Figs 5 and 7A) because they are compose of till deposited in subglacial and ice-marginal settings. Such well streamlined features are attributed to high discharges, and were formed under fully submerged flow conditions (Komar, 1983; Meinsen et al., 2011). By contrast, the elongated ridges in the distal zone of the BOF are further apart than those located in the proximal zone and consist of water-lain GLOF sediments composing the flanks of two parallel scoured channels (Figs 2A, B, 4 and 7B). These ridges in distal setting are interpreted as erosional bars because they are composed of GLOF sediments, but the final morphology of these bedforms was shaped due to lateral scouring of channels separating elongated ridges (Maizels, 1997; Benn et al., 2006; Meinsen et al., 2011).

4.2.2.2. Isolated scours fills

Facies description

Sedimentary successions of isolated scours infills were recognized in the Bachanowo 4 site and along selected reaches of two GPR profiles located in proximal and distal zones of the BOF (Figs 5, 7 and 8; Table 3).

Scour bottoms referring to a basal erosional surface and the scouring depth occur at two morphological levels, i.e. 246 m a.s.l and 244 m a.s.l. in proximal zone of the BOF (Figs 4A, 5A and 7A). Here three types of reflections constitute the set of radar facies of scour infill which reveals maximum thickness as 3.8 m (GPR profile A-A' in Fig. 7A). The lower and middle parts of the scour infill continuous and densely undulated reflections that are locally noisy (RF4). The pattern of the RF4 facies indicates two sedimentary successions, the youngest of which is 3 m thick and which cut previously-deposited sediments of RF4 and substratum (RF1) (Fig. 7A). In the upper parts of scours, very-high-amplitude, wavy and continuous reflections (RF5) appear, capped locally by the sediments of low-amplitude and noisy reflections (RF6).

The radar facies forming the scour infills in the distal zone of the BOF (near the Bachanowo 4 site) are represented by wavy and continuous reflections (RF5) and low and moderate, continuous reflections (RF7) (Fig. 7B). These radar facies lie below a continuous and dense, finely undulated reflection (RF4) and low amplitude and locally noisy reflections (RF6).

The sedimentary succession of isolated scour in the Bachanowo 4 site (Fig. 8; Supplementary 2), is represented by three facies associations (1–3 in Fig. 8). The first is incompletely excavated, showing only horizontally or low-angle stratified sandy medium gravels, which are poorly sorted and have gravelly laminae exhibiting openwork texture and/or sandy interbeddings (GRh(o) and GRl(o) facies; Fig. 8A, C, E; Table 3). These sediments are covered by ripple-cross laminated, fine sands with fine gravel admixtures, which are moderately sorted. The second association (GBm, GRsc/GPsc, GSm, Sr/Sm; 2 in Fig. 8) represents a fully-developed scour infill succession bounded by upper and lower erosional surfaces. The lower erosional surface dips downstream along with a layer of massive gravels with boulders (GBm) of a thickness of up to 0.6 m; its matrix is represented by poorly sorted, sandy medium gravels

(Table 3). Nevertheless, the main sediment body of scour infill represents facies GRsc(GPsc)(o) (Figs 8A, B, E), which changes upward from poorly sorted sandy very fine gravels and sandy medium gravels into very poorly sorted coarse silty sandy very fine gravels (Tab. 3). This succession is up to 1 m thick and reveals crude concave-up and sigmoidal cross-stratificationwith open-work texture (Figs 8D, E). The upper part of facies association 2 comprises two thin and discontinuous sediment layers, and consists of massive diamicton, which is matrix-supported and with a moderate content of clasts (DGm(m_2)), where the matrix is represented by very coarse silty fine sands, very poorly sorted (Fig. 8A; Table 3). The same textural types of sands, but showing massive structure or ripple cross-lamination, composes the second layer, in places capping the diamicton (Fig. 8A-B).

The lower part of the third facies association of a thickness up to 1.2 m comprises massive gravels and boulders (GBm and BCm facies in Fig. 8A, B). The maximum length of longer boulder axes is 0.8 m, while the matrix is poorly sorted sandy medium gravels. These sediments are covered by a discontinuous facies of sinusoidally or low-angle cross-stratified sandy medium gravel (maximum thickness 0.45 m), which is also poorly sorted but exhibits openwork texture (GRl(o)/GRs(o) facies in Figs 8B, F; Table 3). The upper part of the third facies association is completed by massive gravels of a thickness up to 1.1 m with matrix of very poorly sorted muddy sandy gravels (GSm facies in Fig. 8B).

Facies interpretation

The scour origin and evolution were related to the cyclic erosion and deposition of three upward-fining sedimentary successions. The first but incomplete succession (facies association 1 in Fig. 8) is similar to the upper member of the second succession (facies association 2 in Fig. 8) comprising facies GBm→GRsc/GPsc(o)→DGm(m_2)/GSm→SFm/SFr. Its lowermost member (GBm facies) is interpreted as a gravelly lag determining the trough depth. The main (inner) member (GRsc/GPsc(o) facies) represents scour infill deposition (Cartigny et al., 2011, 2014; Lang and Winseman 2013; Lang et al., 2017a, b, 2021), while the upper member (DGm(m_2)/GSm→SFm/SFr), which starts with the dense suspension fall-out (Postma et al., 1988; Lang et al., 2017a, b, 2021; Winsemann et al., 2018), is typical for the final phase of the development of GLOF-related scours in subaerial conditions (Weckwerth et al., 2022). The deposition of scour infill finishes as fine-grained facies (SFm/SFr) capping the scoured riverbed, which coincides with flow being subcritical or even terminating (Carling, 2013).

The third facies association represents a short sedimentary succession defined as GBm/BCm→GRl(o)→GSm, which is dominated by massive, poorly sorted, matrix-supported pebbles and granule-gravels, interpreted as mostly related to rapid deposition in turbulent gravel bedload sheets under high-energy hyperconcentrated flow (Craig, 1987; Maizels, 1993; Cronin et al., 1999; Russell and Marren, 1999; Carrivick et al., 2004; Russell, 2009; Carling, 2013; Peters and Brennand, 2020; Weckwerth et al., 2022). These conditions were interrupted by the development of up-flow migrating antidunes (facies GRl) (Fielding, 2006; Lang and Winsemann, 2013; Lang et al., 2017a, b, 2021).

4.2.2.3. Scour trains

Facies description

The Szeszupka 1 site lies in the northern part of the SOF and within the extent of a scour train (with scour spacing ranging between 34 and 44 m) that comprises three elongated and enclosed depressions (Figs 5E and 9A, B; Table 3). The GLOF sediments forming the scour infill have a thickness of 3.8 m and form four lithofacies associations lying on pre-flood deposits, represented by moderately sorted, planar cross-stratified gravelly sands. The lowermost GLOF facies association (1 in Fig. 9; Supplementary 3) consists of horizontally or low-angle stratified sandy gravels and granules exhibiting openwork texture (GRh(o), GSh, GRl(o)). These deposits are moderately well to poorly sorted (Table 3). Lying above, the second facies association (2 in Fig. 9B–D, G) comprises massive gravels and boulders with sandy matrix (GSm) covered by poorly sorted sandy gravels and granules with crude laminae dipping downstream at low angle (facies GRl/GRh(o)), exhibiting openwork texture and wrapping around the boulder partially buried in GSm facies (Fig. 9A, G; Table 3).

The lower part of the third facies association (3 in Fig. 9) is occupied by massive gravels and boulders (GBm), while co-sets lying above are represented by concave-up gravelly scour infills (GRsc(GSsc)) and backset cross-stratified gravels (Gbl), which often exhibit openwork texture (Fig. 9C–G). The individual scour infill co-set (e.g., GBm, GRsc and SFm/SFh facies in Fig. 9C, E, F) reaches a maximum thickness of 0.9 m, ending with massive or horizontally stratified silty sands (SFm and SFh facies in Fig. 9C, F). The facies GRsc(o) have crude laminae, which are concave-up across the palaeoflow (Fig. 9D, F). Gravelly facies of scour infills are poorly, moderately and well-sorted, while overlying SFm and SFh facies are poorly sorted (Table 3).

The uppermost facies association (4 in Fig. 9) mostly consists of granules exhibiting crude concave-up laminae (GRsc facies) or having massive structure (GRm, GPm, GSm/SGm). These sediments are also characterized by openwork texture or are supported by a matrix consisting of moderately sorted silty sand (Tab. 3).

Facies interpretation

Four phases of sedimentation, referring to sedimentary associations 1–4 (Fig. 9) under conditions of high-energy meltwater outflow to the south, are recorded at the Szeszupka 1 site. The first and the second phase of sediment deposition refer to the rising stage of a GLOF (Fig. 9B). The first phase (facies association GSh, GRh(o), GRl(o), GSh) represents upper-stage plane-bed development with superimposed diminished dunes (Røe, 1987). During the second phase (facies association 2), partially buried boulders formed a lateral depression in a wake and riverbed scour as a result of the development of a relatively small horseshoe-vortex system (Meinsen et al., 2011; Schlömer et al., 2021). Subsequently, lateral scours were infilled by normally graded pebbles and granules with openwork texture (facies GRl(o) in Fig. 9E) as a result of hydraulic clast-size segregation (Carling, 1984, 1990; Lunt and Bridge, 2007; Schlömer et al., 2021) associated with a flow over submerged boulder tops (Carling et al., 2002; Alexander and Cooker, 2016). In general, the upward coarsening sediment deposition from facies association 1 to 2 was accompanied by irregular sediment sorting processes.

The third phase of sedimentary succession is represented by facies association 3 and interpreted as a deposition during the flood peak or near-peak conditions (Fig. 9B) (see Russel, 2007; Cartigny et al., 2014; Lang et al., 2017a, b). The clustered boulder-gravel facies (GBm in Fig. 9A, C) indicates the bases of scouring processes, confirming also the turbulent nature of flow (Kostic et al., 2010; Russel and Knudsen, 1990, 2002a, b; Winsemann et al., 2009; Cartigny et al., 2014; Lang et al., 2017b, 2021; Slootman and Cartigny, 2020), while the amalgamated and stacked scour infills, which are characterised by laminae dipping upstream (Gbl facies) or symmetrically infilling the troughs (GRsc and GPsc facies), correspond to repeated phases of scouring in zones of strong vortices followed by deposition in zones of hydraulic jumps. Such processes are associated with cyclic steps or the development of chute-and-pools (Alexander et al., 2001; Russell and Arnott, 2003; Duller et al., 2008; Cartigny et al., 2014; Lang et al., 2017a, b).

The fourth phase refers to the waning flow stage and final scour infill under conditions of high-concentration suspension fall-out and accumulation of sheets of matrix-supported and poorly sorted gravels or it is indicative of hyperconcentrated flows and rapid deposition (Fig. 9B) (Maizels, 1993; Costa, 1984; Russell and Knudsen, 1990, 1999; Rushmer, 2006; Russell, 2009; Peters and Brennand, 2020).

4.2.2.4. Small-scale pendant bars

Facies description

The sedimentary succession of a pendant bar occurring downstream of a residual hummock (Fig. 5F) was recognised in the Szeszupka 2 site, where two facies associations were distinguished (1 and 2 in Fig. 10; Supplementary 4). The first facies association (Gsc(o), GSm, Ss/Sh) is dominated by scoured medium gravels of thickness greater than 0.8 m with crude wavy laminae dipping downstream (facies association 1 in Fig. 10A–D). These gravels are moderately and very well sorted, displaying openwork texture. Two thin (up to 0.4 m) and discontinuous facies lie above and are represented by massive and poorly sorted gravels and boulders with sandy matrix (GSm) covered by poorly sorted sinusoidally or horizontally stratified, sandy medium gravels (SGs/SGh).

The second facies association is complex (facies GRm/GSm, GBm, Sl/Sh, GS/GRsc, SFm, Sm, SFm) and has an overall thickness up to 1.8 m (2 in Fig. 10), which corresponds with the height of the pendant bar located on the downstream side of an elongated ridge (Fig. 5F). The dominant facies are massive, poorly sorted and represented by fine gravels with admixture of boulders and with sandy matrix (GRm/GSm and GBm facies in Fig. 10). These sediments are interbedded by facies of scoured sandy gravels (GS/GRsc) or low-angle and horizontally stratified, slightly gravelly sands (SGh and SGl facies), which are moderately sorted. The upper part of the second facies association comprises very fine sandy, very coarse silt and fine sands, which are slightly very fine gravelly and have admixture of very fine silt. These sediments form SFm and Sm facies, which are of massive structure (Fig. 10A, B, G).

Facies interpretation

The development of the small-scale pendant bar was controlled by changes in the morphology of the outburst fan surface during the waning flood stage and relates to intense turbulence that led to pool scouring followed by two-stage deposition. The scouring processes were associated with the hydraulic jump zone located downstream of the elongated ridges (Komar, 1983; Meinsen et al., 2011). The first stage of deposition resulted in trough infilling by gravels with convex-up and downstream-dipping laminae (Fielding, 2006; Duller et al., 2008; Cartigny et al., 2011, 2014; Lang and Winseman, 2013). The intensive outwash of a fine fraction under the condition of a Froude-supercritical flow regime caused the dominance of openwork texture (Carling, 1984, 1990; Lunt and Bridge, 2007; Slootman and Cartigny, 2020). The length and morphology of the distal portion of the submerged elongated ridge were constantly modified due to flow acceleration, causing upstream migration of the scour. Progressive scour displacement allowed the development of a reattachment zone in the near wake, where the second stage of deposition occurred (Sutton and Neuman, 2008; Neuman et al., 2013; Lekkala et al., 2022). The thickness of facies association 2 (Fig. 10) refers to the bar height, and hence constitutes the main sediment body of the pendant bar, documenting its development in the near wake (second stage of deposition). The deposition of facies GRm/GSm, GBm points to the unstable structure of the secondary flows, which changed from the supercritical flow sufficiently for sand to separate from gravels to the suspension fall-out and accumulation of sheets comprising matrix-supported, poorly sorted gravels (Craig, 1987; Maizels, 1993; Rushmer, 2006; Hornung et al., 2007; Russell, 2009; Carling, 2013; Peters and Brennand, 2020). The abrupt changes in flow competence concerned the less energetic conditions and more fluid flows when sandy upper plane bed or up-flow migrating antidunes (Sl/Sh facies) or even scours in the zones of hydraulic jumps (facies GSsc/GRsc(o)) were formed (Figs 10A, B) (Fielding, 2006; Lang and Winsemann, 2013; Lang et al., 2021). Finally, fine-grained sediments of massive structure (SFm, Sm facies) topped the pendant bar when the flow rate declined (Russel et al., 2003; Carling, 2013).

4.2.2.5. Small-scale chute bars

Facies description

At the Bachanowo 3 site, sedimentary unit U1 consists of two facies associations (1 and 2 in Fig. 11A; Supplementary 5), followed by unit U2, both separated by erosional contact. The first facies association in unit U1 is represented by scoured, very fine gravelly, coarse sands, which are poorly sorted (1 in Fig. 11A). These sediments are covered by a facies association comprising three sedimentary rhythms (2 in Fig. 10A). The first of them (GSs/Ss, GRh(o)) has a thickness up to 1.4 m. Here, the lower facies (laminae) are represented by gravels with massive or stratified sandy matrix, clast supported, while the upper facies are composed of sands or granules with openwork texture. In general, these poorly and very poorly sorted sediments forming an upward coarsening sedimentary succession with laminae representing sheet-like beds dipping downstream at a low angle (10–12°) (Fig. 10A, B). Their primary stratification is deformed by normal faults dipping also downstream at 13–64°.

The second sedimentary rhythm (GRs(o)/SGs) comprises sinusoidally stratified, normally graded granules with openwork texture (lower layer) and sands with admixture of gravels, clast supported (upper layer), and both discontinue but without gravitational deformations. The bounding surfaces of this rhythm dip downstream at 8° (Fig. 11A, C). These sediments represent an upward coarsening succession, with sorting that changes from poor to very poor.

The third sedimentary rhythm has a 1.5-m thickness and is characterised by sheet-like sandy beds dipping downstream at 8–10°, in which the sedimentary succession displays changes in stratification type, from horizontal to sinuous (SGh/Sh/Ss→SGs/Ss) (Fig. 11A, D–E). These sediments progressively grade upward, from very fine gravelly medium sand, poorly sorted at the base, throughout medium gravelly fine or medium sands, into moderately sorted slightly very fine gravelly fine sand (facies SGs/Ss). Moreover, redeposited soft-sediment clasts (rip-up clasts) consisting of glacial till are noted, above which Ss facies occurs (Fig. 11A, E).

The succession of three rhythms in the Bachanowo 3 site is capped by facies association GSm, Sm, constituting sedimentary unit U2 of a thickness up to 0.9 m (Fig. 11A, F). Its lower member is massive, poorly to very poorly sorted medium gravels with sandy matrix (GSm facies; $14.7 \leq d_{50} \leq 15.6$), while the upper one is massive and very poorly sorted, slightly gravelly, sandy mud (d_{50}=0.05 mm).

According to the pattern of radar facies recognised in the distal reach of the chute bar, the thickness of its sediments decreases from 3.6 m to 2 m over a distance of 47 m. The distal portion of the chute bar comprises radar facies characterised by very high amplitude, wavy and continuous reflections (radar facies RF5) and strong, continuous and finely densely undulated reflections (radar facies RF4), interbedded by a thin layer of RF7 characterised by planar and locally wavy noisy and moderately continuous reflections (Fig. 7B). A similar radar facies type (RF7), but comprising more continuous and wavy-dominated reflections, occurs within the extent of the chute bar and scoured channel, and has a thickness up to 2.5 m (Fig. 7B).

Facies interpretation

The fan-shaped, small-scale chute bar was formed after the bed scouring and followed by the deposition in hydraulic jump zones (radar facies RF2 capped by RF7 and GSsc facies in the Bachanowo 3 site, respectively). Chute bar origin refers to the three-stage vertical accretion, and each stage is represented by the rhythmically bedded gravel and sand couplets deposited by repeated flow pulses (Russel and Knudsen, 1990; Carling, 2013). At the first stage, the steady stresses were responsible for producing inversely graded gravel–sand couplets, i.e. rhythm GSs/Ss(GRh(o)) (Sallenger, 1979; Hiscott and Middleton, 1980; Lowe, 1982), and their high accumulation rate was associated with antidunes formation The identified out-sized clasts (cobble-size) suggest flow conditions above upper-stage plane beds (Russel and Knudsen, 2002a, b) or, alternatively, deposition from hyperconcentrated flows (Postma et al., 1988; Russel and Knudsen, 1990, 2002a, b). Progressively, the increase in the thickness of gravelly beds at the expense of the thickness of sandy layers observed in couplets indicates a decrease in the frequency and duration of weak flows. In addition, such high-aggrading beds were deformed by downstream-dipping normal faults as a result of their dewatering.

In the second stage (sedimentary rhythm GRs(o)/SGs), the flow conditions were more stable. The crude sinusoidal stratification indicates a more fluid phase, while its openwork texture resulted from increasing flow turbulence (Carling, 1984, 1990; Lunt and Bridge, 2007; Slootman and Cartigny, 2020). Considering this, the morphology of the downstream inclined surface of the chute bar was dominated by antidunes formed under the condition of a Froude-supercritical flow regime (Carling, 1984, 1990; Lunt and Bridge, 2007; Slootman and Cartigny, 2020).

Rhythmic bedding of normally-graded sands and fine gravels (finer than the sediments lying below) characterise the third stage in chute bar evolution. Till clasts grounded on the surface of a chute bar caused small hydraulic jumps to form (Ss facies in Fig. 11E). During the flood recession, the sand-dominated Froude-supercritical plane bed changed into small antidunes formed under pulsed outflow (succession SGh/Sh→SGs/Ss).

Finally, the chute bar surface was transformed after the GLOF sedimentation (post-GLOF unit U2), as a meltwater outflow was responsible for the deposition (following erosion) of gravel bedload sheets (GSm and SGm facies) topped by the fine-grained sediments of massive structure (Sm facies) as flow rate declined. The deposition of unit U2 and the reworking of the chute bar surface occurred when the Szeszupa Tunnel Valley was occupied by remnants of dead ice, which in general prevented this depression from being filled by the outwash deposits. The post-GLOF deposition of unit U2 most likely was related with the development of eskers superimposing the GCLs near Łopuchowo, as an initial phase of dead-ice topography development in the Szeszupa Tunnel Valley (Figs 2C, 12 and 13).

4.2.3. The ages of the outburst fan sediments

The ages of outburst fan sediments were determined for two sites documenting the internal structure of isolated scour infill (the Bachanowo 4 site: OSL samples 20011 and 20012; Fig. 8A) and sedimentary succession of the chute bar (the Bachanowo 3 site: OSL samples 20009 and 20010; Fig. 11A). Doses reveal a wide span between 33.1±2 Gy and 159.4±14.4 Gy (samples 21010 and 21012, respectively) along with relatively wide values of dose rates between 1.54±0.07 Gy/ka and 2.45±0.10 Gy/ka (21011 and 21010, respectively).

The wide range of D_e's and dose rates resulted in a wide range of mean ages between 13.5±1.0 ka and 106.6±7.7 ka. The model preference (Arnold et al., 2007) was applied, and assuming a p-value close to zero for all samples, the Central Age Model (CAM) was used, giving only slightly younger ages of between 102.3±7.8 ka and 13.2±0.9 ka. The Bachanowo 3 sediment profile revealed ages of 25.5±2.5 ka and 13.2±0.9 ka – much younger than the Bachanowo 4 profile.

Assuming that the dose distribution of the 21010 sample is the only one with low skewness value (σ=0.03), the age of 13.2±0.9 ka must be considered as effectively bleached and the most reliable in our dataset. This result means that the age of 13.2±0.9 ka is a reliable date for the uppermost part of the Bachanowo 3 profile. Complete bleaching of the rest of the samples (21009, -11 and -12) might be questionable and is discussed in a wider context further in the text.

5. Discussion

The interpretation of the geomorphological data enabled the identification two types of floodwater outlets, which evolved during the GLOF at the end of the last glaciation. Their development is presented and discussed here in the context of ice-margin behaviour and flooding events. The proposed conceptual model covers the evolution of these outlets and associated outburst fans, and it consider the flow stages of a subglacial-lake outburst flood and mutual interactions between floodwater outlets as they evolved, which also played a role in the origin of outburst fans. We also discuss factors that control the origin of small-scale bedforms on the outburst fan surface and that were inferred from both sedimentological and geomorphological data. However, one should bear in mind the limitations of the interpretations, which results from the lack of large sediment exposures and the relatively small size of the trenches, which may hamper the recognition of sedimentary structures.

5.1. Types of floodwater outlets

The Bachanowo Gate represents a completely preserved floodwater outlet zone (Figs 1–3). This interpretation is supported by the existence of a submarginal landforms continuum as GCLs→initial GCLs→ITZ that developed on a gradually adverse dipping subglacial bedslope and at the contact with the outburst fan apex. In the case of the SOF, the formation of supraglacial fracture outlets (the Szeszupka Gate in Fig. 12A, C) and hydraulic jacking (Roberts et al., 2000a, b; Gomez et al., 2002; Waller et al., 2001) is supported by (1) up-ice dipping of proximal margin of the Szeszupa Tunnel Valley, (2) the preservation of only the distal part of the SOF and (3) the origin of the GCLs in the Wodziłki sub-basin linked with the development of outburst terraces T2 and T3 (younger than the SOF) in the Western Spillway (Fig. 12). Considering the morphology of the submarginal zone near the SOF, floodwaters flowed up an adverse slope that exceeded the ice-surface slope by more than 4.9-, 3.2- and 2.4-times (in terms of degree angle) taking into account various values of the A coefficient in the ice-sheet surface calculation (A=1, A=1.5 and A=2, respectively; Fig. 12), which is favourable for glaciohydraulic supercooling (Alley et al., 2003; Larson et al., 2006). The supraglacial fracture forming the Szeszupka Gate had a length up to 2.3 km and was located at distances at least 1.5–2 km from the terminus and aligned perpendicular to the Szeszupa Tunnel Valley axis (Fig. 12A, C). In view of the jökulhlaups in Iceland, the Szeszupka Gate was probably in the form of a supraglacial depression characterised by a steep headwall and up-glacier dipping floor morphologically related to hydrofracture transformation due to changes in water pressure (Russel and Knudsen, 1999; Roberts et al., 2000b; Waller et al., 2001; Gomez et al., 2002). All in all, the SOF sediments were most likely deposited by previously supercooled meltwater flows that ascended from the base of the over-deepened, main (axial) part of the tunnel valley (the Szeszupa Tunnel Valley) via high-angled hydrofractures (cf. Roberts et al., 2000a, b, 2001; Russell et al., 2006, 2007). This interpretation means that the SOF evolved as a supraglacial outlet, while the BOF was formed when the subglacial flood was enlarged to the western flank of the Szeszupa Tunnel Valley, and when floodwater outlets were able to divert parallel to the ice front and rapidly spread across the glacier snout (cf. Gomez et al., 2000; Roberts et al., 2000a, b, 2001). These processes finally caused the reduction of subglacial water pressure due to the establishment of a new outlet of subglacial floodwaters, i.e. the Bachanowo Gate (Fig. 12A) (cf. Russel et al., 2010). Probably at the same time, the Szeszupa Tunnel Valley was also drained to the south by the Jeleniewo Tunnel Valley (Fig. 12A), feeding the Prudziszki Gate (Weckwerth et al., 2019; Figs 1A, B and 12).

5.2. Ice-margin behaviour as a consequence of floodwater outlets development, changes in flood discharge and flooding events

The GLOFs were capable of forming a subglacial channel in association with a specific lake storing meltwaters (e.g., Kirkham et al., 2022). Such a subglacial reservoir in topographically confined basins probably developed in south-western Lithuania, between Jurgežeriai, Bilvyčiai and Krasna, and meltwaters were repeatedly funnelled into the Szeszupa Tunnel Valley (Weckwerth and Wysota, 2024). These meltwater activities support the glacier bed erosion due to highly dynamic subglacial flow at a peak discharge that also covered the flanks of the Szeszupa Tunnel Valley (Fig. 12A, C).

Considering the morphological data, the BOF and SOF and associated outlets (gates, portals) developed during at least two GLOFs. Initially, the Szeszupka Gate evolved first under conditions of the rising stage or even at the initial phase of peak discharge during the first GLOF

(GLOF1 in Fig. 12). Its rising stage started also with erosional processes that resulted in the formation of an ice-walled gorge (canyon), providing room for fan deposition and the development of bedforms. The Szeszupka Gate represents a supraglacial fracture outlet, confirming the existence of basal water pressures in excess of the overburden pressure during the initial stages of the flood (see Roberts et al., 2000b; Waller et al., 2001; Russel et al., 2010). Such interpretation means that the Szeszupka Gate must have existed only when the Bachanowo Gate was not active, particularly because the latter is located at the lower elevation and both gates have the same subglacial feeding system (the Szeszupa Tunnel Valley) (Fig. 12). Moreover, the existence of a supraglacial fracture outlet (the Szeszupka Gate) indicates a symmetrical or even asymmetrical GLOF hydrograph with a rapid rise to peak discharge (Roberts et al., 2000b; Rushmer et al., 2002). Further confirmation of the duration of the rising flood stage being shorter than the waning one is provided by the bedforms evolved on both the SOF and the BOF during the waning flood being more diverse than during its rising phase (Maizels, 1997; Rushmer and Russel, 2002; Russel and Knudsen, 2002a, b; Russel et al., 2006). Conversely, increased erosion during the waxing stage of flow may lead to limited bedforms preservation and thus the shape of the presumable GLOF hydrograph may seem to be debatable. Moreover, the pulse-like fluctuations of the flow near the peak discharge of the GLOF1 were possible, causing repeated erosion during the development of chute-and-pools in the ITZ and on the BOF surface, which was marked by cyclically formed boulder lags in the isolated scour (Bachanowo 1 and 4 site; Figs 6 and 8A) (Kozlowski et al., 2005; Russel et al., 2006). Such fluctuation in the flood hydrograph may also reflect the formation of temporal constrictions in the subglacial drainage conduit (e.g., Clarke et al., 2004), which was possible on the western flank of the Szeszupa Tunnel Valley during the peak discharge, when the propagating hydraulic waves caused rapid temporal and spatial switching of submarginal bed erosion (Russell et al., 2001; Blauvelt et al., 2020; Wells et al., 2022; Harrison et al., 2023). This process resulted in the Bachanowo Gate forming and lateral enlargement of the Szeszupa Tunnel Valley, when the outburst flood neared peak discharge (Fig. 12A) (Roberts et al., 2000a, b; Russel et al., 2006).

Multi-channelized drainage evolved in the submarginal zone close to the Bachanowo Gate, reflecting the phase of subglacial flood discharge that followed the pressurised sheet flow (Shoemaker, 1992; Björnsson, 1998; Roberts et al., 2000b; Russell et al., 2006). Here, the rapidly decreased ice thickness affected the existence of the submarginal landforms continua (GCLs→initial GCLs→ITZ), which reflects the erosion ability being decreased by multi-channelised subglacial meltwater (Lesemann et al., 2014), replacing multi-channelised drainage by pressurized sheet flows in the ITZ close to the Bachanowo Gate (Fig. 12A, C). The occurrence of intraclasts in the ITZ (Bachanowo 1 site; Fig. 4) confirms (1) the high-capacity drainage and erosion at the submarginal position, (2) the intense turbulence and rip-up processes of the unconsolidated and unfrozen ice-sheet bed under the ice-sheet margin (Postma et al., 2009, 2014; Ito et al., 2014; Lang et al., 2017a) or (3) the existence of permafrost preventing floodwater drainage through the bed (Russell et al., 2001; Roberts et al., 2001; Lesemann et al., 2010, 2014; Tylmann, 2014; Adamczyk et al., 2022). Subsequently, the sediment deposition here was unstable, according to the short-term fluctuations in flow energy as a response to pulses in water pressure (i.e., Kavanaugh and Clarke, 2000). Nevertheless, the fracturing of the glacier snout along the Bachanowo Gate was associated with the pressure of water exiting a portal within the ice and the rapid release floodwater which broke the ice blocks off (Roberts et al., 2000b, 2001; Russel et al., 2006). The existence of deformations associated with ice-block degradation occur only in the intermediate zone (ITZ) at the contact with the BOF apex, but not in sedimentary successions of bedforms in more distal settings of outburst fans, and may confirm the relatively low volumes of ice blocks indicative of a sedate rising stage of the GLOF1 (see Russel et al., 2006).

The second event (GLOF2; Fig. 12) was related to the formation of GCLs in the Wodziłki sub-basin that lies at a lower position than those near Łopuchowo (Figs 1, 2 and 12).

This second burst was drained only through the ice portal intersecting the SOF (the inactive Bachanowo Gate), allowing the development of the Wodziłki sub-basin and terraces T2–T3 in the Western Spillway (Fig. 12B) (cf. Maizels, 1997; Russell and Knudsen, 2002a, b; Rushmer, 2006). Such an interpretation allows the presumption that the bottom of the southern end of the Szeszupa Tunnel Valley was scoured by at least two bursts forming the subglacial basins and GCLs (Fig. 12A, B) (Piotrowski, 1994; Jørgensen and Sandersen, 2006; Fleisher et al., 2010; Kehew et al., 2012).

5.3. Factors controlling the origin of small-scale bedforms

The role of proglacial topography in the development of ice-marginal fans and proximal reaches of outwashes formed by the GLOFs has frequently been investigated in terms of sediment transportation and deposition influenced by a sediment flux and backwater level changes under confined or semi-confined settings (e.g., Russel and Knudsen, 1990, 2002a, b; Russel et al., 2006). Backwater level changes were not a control in the development of the BOF and SOF, because both evolved in laterally confined settings of the proximal portion of the Western Spillway in the form of an ice-walled canyon (Figs 1C and 12A, B). The distal portions of the BOF and SOF widened because of flow radiating from the Bachanowo and Szeszupka outlets on the waning flow stage. Thus, the morphology of the outburst fans is characterised by the erosional surface with superimposed depositional bedforms developed in a laterally confined setting. Such a setting controlled the sedimentary processes in the Gígjukvísl ice-walled canyon in Iceland, but, in that case, outburst fans developed in the front of this canyon (Russell and Knudsen, 1999a, 2002b; Russel et al., 2006). Nevertheless, Russell and Knudsen (1990) highlighted proglacial trench morphology as the control on outwash sedimentology.

In the case of the BOF, floodwater drained directly from the mouth of the subglacial channel onto the fan surface, the width of which increases downstream (Figs 1, 2 and 12A). Its two morphological levels are associated with different flow stages (Figs 3 and 12). The elevated and concave-up proximal zone reflects the prevailing rising stage, while the lowered distal zone, with uniform surface gradient as in the case of the SOF surface (Fig. 12), represents the waning stage and processes of flow channelisation and fan surface dissection (falling-stage-dominated fan; cf. Russel and Knudsen, 2009a, b; Russel et al., 2006). Moreover, the narrow proximal zone of the BOF is dominated by the erosional downstream-elongated ridges (residual hummocks) and occasional scours, while the wide distal zones of both fans stand out for downstream decreasing in number of residual hummocks and scours and abundance of pendant bars, distributive channels and chute bars (Figs 2, 4, 13 and 14). Such changes in proximal–distal bedform types and associated lithofacies (landform–sediment continuum; cf. Wells et al., 2022) on an outburst fan surface in a laterally confined setting is observed regardless of the feeding systems of the outburst fans at the submarginal position (multichannelised subglacial flow and up-ice dipping fractures for the supraglacial outlet for the BOF and SOF, respectively; Fig. 12A, C).

Sedimentary processes and bedform origins on outburst fan surfaces are usually associated with fluctuations in meltwater discharge and changes in sediment supply (Russel and Knudsen, 1990, 2002a, b; Russel, et al., 2006; Harrison et al., 2023). The existence of well-developed GCLs, an over-deepened distal part of the Szeszupa Tunnel Valley and the development of a proglacial trench (ice-walled canyon) laterally confining outburst fans indicate highly effective subglacial and proglacial erosion causing high sediment concentration of the GLOF. Intraclasts identified in submarginal and proglacial settings suggest erosional processes whether at rising or waning stage (Russel, et al. 2006). However, downstream decreasing in the peak discharge or changes in the flow stages, over time influencing the sedimentary environment, resulted in the development of bedforms and a sediment continuum on the outburst fans (Figs 13 and 14; Table 3).

5.4. Sedimentary processes in bedform origins

Processes of erosion, transportation and sediment deposition controlled by the morphology of the ice-walled canyon, downstream distance from floodwater outlet and flow stages all play a crucial role in bedforms development and their spatial (downstream) distribution on the surface of an outburst flood fan (Russell et al., 2006; Marren and Shuh, 2009; Winsemann et al., 2011, 2016, 2018; Carling, 2013; Lang and Winsemann, 2013; Weckwerth et al., 2019, 2022; Lang et al., 2021; Wells et al., 2022). The recognised landform–sediment continuum on an outburst fan surface in a laterally confined setting, comprising proximal and distal fan zones, starts with the development of streamlined erosional residuals, scours and their trains and, finally, small-scale pendant bars, distributive channels with erosional bars and small-scale chute bars (Table 3; Figs 13 and 14).

5.4.1. Downstream-elongated ridges

Downstream-elongated ridges (streamlined erosional residuals) are considered as diagnostic for glacial lake-outburst floods (Baker, 1973; Kehew and Lord, 1986; Lord and Kehew, 1987; Maizels, 1991; Kehew, 1993; Kozlowski et al., 2005; Benn et al., 2006; Wells et al., 2022). These ridges recognised on the BOF and SOF represent (1) equilibrium residual hummocks, the morphology of which was adjusted to minimise resistance to flow in the proximal zone of the outburst fan (Baker, 1978; Komar, 1983, 1984; Kehew and Lord, 1986; Benito, 1997) and (2) erosional bars comprising vertically accreted GLOF sediments but finally shaped under conditions of waning floodwater outflow in distal fan (Maizels, 1997; Benn et al., 2006). Both types of downstream-elongated ridges are characterised by usually higher values of the aspect ratio (average 5.8 and 5.5 for the BOF and SOF, respectively) than streamlined hills recognised in NW Germany (average 3.3) (Meinsen et al., 2011). Considering the results of earlier studies showing that the aspect ratio between 3 and 4 refers to streamlined bedforms providing the least amount of resistance to the water that formed them (Baker, 1978; Komar, 1983), it cannot be ruled out that the high values of this ratio for the BOF and SOF reflect processes of post-GLOF fluvial reworking (Fig. 14B). Such water activity was recognised for chute bar transformation (unit U2 in Bachanowo 3 site; Fig. 11A, F). Nevertheless, well-streamlined bedforms may indicate continuous long-term flooding (Kehew et al., 2009), and, before post-flood reworking, formation under submerged flow conditions because they represent the smallest and highly elongated features (cf. Meinsen et al., 2011).

The equilibrium residual hummocks in the proximal fan refer to the onset and rising flood stage (Fig 14A) when the increasing discharge was powerful enough to form a proglacial trench and to scour an unconsolidated substrate under high discharge conditions. The existence of such hummocks in the BOF proximal zone affected flow separation until the very end of the flood and shallow channelisation under lower energy conditions (see Benito, 1997). As an effect, during the final stage of streamlined features development, these acquired a high value of the length/width ratio (average 5.8 and 5.5 for the BOF and SOF, respectively) (cf. Komar, 1984; Benito, 1997).

In the distal zone of both fans, downstream-elongated ridges are interpreted as erosional bars (Fig. 14A, B). Here, the lack of one major incised channel suggests high sediment flux confirmed also by the openwork texture commonly characterising the distal fan scour infills in the Bachanowo 4 and Szeszupka 1 sites (cf. Russell and Knudsen, 1999, 2002a, b; Fay, 2002; Russell et al., 2006). Moreover, the uniform surface gradient indicates the waning flow stage and its characteristic fan morphology with a complex system of downstream-elongated ridges.

5.4.2. Isolated scours and their trains

Processes forming isolated scours on the BOF and SOF surfaces represent pulses of floodwater outflow neared peak discharge (Kozlowski et al., 2005; Russel et al., 2006; Cartigny et al., 2011, 2014; Lang and Winseman, 2013; Lang et al., 2017a, b, 2021; Weckwerth et al., 2022).

These bedforms represent chute-and-pools, and their repeated development (Russell and Arnott, 2003; Winsemann et al., 2009; Cartigny et al., 2014; Lang et al., 2017b, 2021) comprised riverbed erosion and boulder lag formation followed by successive scour infill (Maizels, 1993; Russell and Marren, 1999; Rushmer et al., 2002; Carrivick et al., 2004; Hornung et al., 2007; Carling, 2013; Peters and Brennand, 2020). The repeated phases of such processes denote a more fluid environment, in which sedimentation occurred as a result of progressive decline in discharge (Hansen et al., 2020; Weckwerth et al., 2022). As a result, the depression in the scoured riverbed was infilled by sediments as the flow regime changed from supercritical-flow-related sedimentation (antidunes and humpback dunes) to subcritical (ripples) (Carling, 2013).

Furthermore, scours form linear clusters on the fan surfaces and are interpreted as a result of upstream-migrating cyclic steps with hydraulic jumps in the intervening troughs (e.g., Lang et al., 2017b, 2021; Slootman and Carigny, 2020; Weckwerth et al., 2022). The initial conditions favourable for their development include (1) the proglacial trench (or ice-walled canyon) laterally confining both the BOF and SOF, which encourage different types of cyclic steps (Strong and Paola, 2008; Winsemann et al., 2011, 2018; Muto et al., 2012; Kostic et al., 2019), (2) rapid changes in initial slope occurring between the glacier snout where supraglacial floodwater outlet existed (the Szeszupka Gate) and its forefield and (3) flow perturbation caused by small-amplitude humpback, diminished dunes or bed obstacles (e.g., partly buried boulder or older scours; cf. sedimentary succession in the Szeszupka 1 site; Fig. 9) (Lang and Winseman 2013; Cartigny et al., 2014; Lang et al., 2017b, 2021; Slootman and Carigny, 2020; Weckwerth et al., 2022). Taking into account the above-mentioned conditions, linear cluster of scours floored by gravels and boulders (GBm facies in Fig. 7C, E, G) and superimposed facies represent progradational scours infills in the zones of hydraulic jumps under conditions of rising flow stage or peak discharge (Maizels, 1993, 1995; Russell and Knudsen, 2002b; Russell et al., 2006). All in all, the topography-controlled occurrence of scour-and-fill events resulted in the development of cyclic steps (e.g., Lang et al., 2017b, 2021; Slootman and Carigny, 2020). These indicate widespread surficial scouring as was reported for Icelandic jökulhlaup fans developed in the front of an ice-walled canyon, which were subjected to high sediment flux on the rising and falling flow stage (Rushmer et al., 2002; Russell and Knudsen, 2002b; Russell et al., 2006).

5.4.3. Small-scale bar formation

The development of depositional features on the GLOFs surfaces was associated with changes in the morphology of floodwater subglacial routeways, which finally affected the changes in the flow pattern (e.g., Baker, 1973; Russell, 1992, 2007; Benito, 1997; Maizels, 1997; Russell et al., 2000, 2006; Carling et al., 2009b; Carling, 2013; Hanson and Clague, 2016). Thus, the transformation of the outburst fan surface by floodwater erosive impact at the rising stage and during the peak discharge created at first the accommodation space, the geometry of which together with the following progressive decrease in flow energy determined the sedimentary processes responsible for the development of bars at the waning stage.

Small-scale pendant bars represent depositional features considered to be evidence for GLOFs and are typical for scabland channels (Malde, 1968; Baker, 1978; Benito, 1997; Kehew et al., 2009; Høgaas and Longva, 2016). These features correspond in shape and location to tails formed at the downstream end of streamlined hills and developed under submerged flow conditions and during waning flows (Komar, 1983; Meinsen et al., 2011). Moreover, the origin of small-scale pendants is attributed to the transition between steep and confined segments and wide reaches of spillways (O'Connor, 1993; Kozlowski et al., 2005; Baker, 2009; Carling et al., 2009b; Marren and Schuh, 2009; Carling, 2013; Winsemann et al., 2016), where the local bed topography and the spillway morphology generated flow patterns that led to deposition. Such conditions occurred more frequently in the distal zone of the BOF and SOF as an effect of erosion decreasing and being replaced with a deposition tendency at the waning stage. Taking into consideration the SOF and BOF location and morphology, the pendant bars identified here represent small-scale features placed on the lee side of elongated ridges that formed flow obstacles (cf. Meinsen et al., 2011; Høgaas and Longva, 2016). As a result of distal scouring of lee-side wake vortices (Krzyszkowski, 2002), pendant bars on the outburst fan surfaces developed in deeper areas located just downstream of flow obstacles (Figs 4 and 14). Hence, the formation of scours on the lee-side of elongated ridges can be assumed as favourable conditions prone to unstable deposition characterised by abrupt changes in flow competence as the bed morphology changed abruptly between gravelly bed sheets, sandy upper plane bed, antidunes and scours formed in the zones of hydraulic jumps (see Komar, 1983; Meinsen et al., 2011). Similar variable or changing flow conditions at the downstream end of the bar were typical for pendant bar development, but small-scale pendant bars do not comprise large-scale planar cross-stratified poorly sorted gravels (cf. O'Connor, 1993; Winseman et al., 2016), which were recognised in the chute bar located on the BOF surface (Figs 5 and 10).

The formation of small-scale chute bars was limited to the zones where flows opened out from the channels separating the downstream elongated ridges at the very end of waning stage flows (Russell et al., 2000, 2006; Russell, 2007). The duration of meltwater waning flow controlled both the intensity of channel incision and, simultaneously, accumulation in zones where floodwater decelerated as it flowed out of a constriction and expanded to the channel widening, forming lobate bars (Shakesby, 1985; Elfström, 1987; Russell, 1993, 2007). These features represent short-lived deposition of fining-upward successions (Fig. 11) under conditions of pulsed and progressive reduction in the flow energy under Froude-supercritical flow conditions (Russel and Knudsen, 1990). The sedimentary rhythms forming chute bar succession confirm high-concentration flow depositing via traction carpets (Nemec and Muszyński, 1982; Carling, 2013).

5.5. OSL age determination for outburst fan sediments

Two dated profiles reveal age consistency, where the result of 64.4±6.3 ka postdates 102.3±7.8 ka in profile Bachanowo 4 (sediments deposited at the final phase of scour infill, waning stage; Fig. 8A), and 13.2±0.9 ka postdates 25.5±2.5 ka in Bachanowo 3 (Fig. 11A). From a sediment perspective, the youngest date of 13.2±0.9 ka likely marks a separate event (sedimentary unit U2), related with “normal” meltwater outflow. This result is considered reliable from a technical perspective, because of its nearly symmetrical dose distribution (Sk=0.03) and the lowest overdispersion (OD=25%±5%) among samples. From a regional perspective it seems reliable, because it is supported by the fact that topped post-GLOF sediments deposited at 13.2±0.9 ka overlap with the youngest cosmogenic ^{36}Cl-exposure age of 14.4±1.0 ka noted for similar geomorphological setting (Dzierżek and Zreda, 2007; Rinterknecht et al., 2005, 2006, 2008) and sediments of an episodic flow at the margin of the adjacent Lipowo palaeolake (Rychel et al., 2023). Our result further postdates the uppermost sedimentary unit comprising glaciogenic deposits in the adjacent Osinki key site dated back to ~15.3–15.0 ka (W. Wysota, personal communication, 2024), along with deposition of sediments forming the GLOF-related megadunes, which took place between 16.9±0.9 ka and 18.8±1.3 ka (sites located south of Bachanowo, south of Suwałki), according to the newest study (E. Kalińska, personal communication, 2024).

The age of chute bar sediments on the BOF surface (25.5±2.5 ka; Fig. 11) is slightly older than expected, and they include some quartz particles that had not experienced proper bleaching. According to Duller et al. (2008), checking the aliquot distribution in small aliquot samples (as in this study) helps in distinguishing proper sediment bleaching. A relatively large dose skewness of 0.63 for the 21009 (25.5±2.5 ka; Fig. 11) agrees with this statement. Rejuvenating this age by a minimal age model, an age of 12.7±1.1 ka is obtained, but the low probability value hampers its usage (Table 2).

The oldest two samples representing isolated scour infills (64.4±6.3 ka and 102.3±7.8 ka; Fig. 8A) carry a significant skewness value of their dose distribution too, and thus their sediment, too, may be not bleached.

6. Conclusions

Two outburst fans in the Suwałki Lakeland, north-eastern Poland originate from a sudden release of meltwater from two types of outlets. The morphology of the ice-contact outwash fans is highly varied, depending upon floodwater outlet types and pre-GLOF proglacial topography. The rising stage and peak discharge caused the erosional processes to predominate, resulting in ice-walled canyon formation, which provided room for fan deposition and bedform development during the flood waning. All the above led to the outburst fans' morphology being characterised by the occurrence of an erosional surface with superimposed depositional bedforms developed in a laterally confined setting.

The supraglacial outlet (the Szeszupka Gate) developed first and was related with glaciohydraulic supercooling and hydrofracturing during the rising stage of meltwater burst (GLOF1) at the southern end of the Szeszupa Tunnel Valley. The associated Szeszupka outburst fan was preserved as only the distal zone of such a feature because the proximal reach existed on the ice-sheet snout due to supraglacial outflow feeding this fan. The Bachanowo outburst fan and the Bachanowo Gate were formed due to subglacial multi-channelised meltwater burst (GLOF1) and started to exist during the pulsed peak discharge, being finally transformed during the flood waning stage. Such processes were associated with the widening of floodwater subglacial routeways, causing deactivation of the supraglacial outlet when floodwater outlets can divert parallel to the ice front and rapidly spread across the glacier snout. These observations lead to the conclusion that, during GLOF1, two outburst fans developed, though asynchronously (corresponding to two different stages of the flood). Further surface transformation of the Szeszupka fan took place during GLOF 2.

GLOF-related small-scale bedforms could form continua in terms of their spatial (downstream) and temporal changes in sedimentary environment, referring to the sediment flux, flood magnitude and its rising or falling stages. During the flood, at submarginal position, there evolved a landform continuum of GCLs→initial GCLs→ITZ, displaying an erosion ability that was being decreased by channelised subglacial meltwater and replaced by pressurised sheet flows close to the floodwater outlet. The small-scale bedforms continuum on the outburst fan surface is associated with the progressive development of streamlined erosional residuals, scours and their trains during the rising stage and peak discharge, while the waning stage and very end of flood conditions were favourable to the formation of pendant bars, distributive channels with erosional bars and chute bars, regardless of the feeding systems of the outburst fans, i.e. channelised subglacial flow for the BOF and up-ice dipping fractures for the supraglacial outlet for the SOF.

The results of OSL dating of outburst fan sediments reveal a limited sediment exposure to the sunlight while deposited, for example in deep floodwater outflow and/or sediment concentration in the water column, and even during the waning stage. Thus, the flood age determination as older than 13.2 ka, based on the age of sediment topping the flood-related features, seems to be the most reliable.

Acknowledgements

We are thankful to two anonymous reviewers for their helpful and valuable comments that improved the quality of the paper. We thank Michał Dąbrowski for help in the GPR profiling. This study was carried out as part of a scientific project financed by the National Science Centre, Poland (project No. 2018/31/B/ST10/00976).

References

Adamczyk, A., Wysota, W., Piotrowski J.A., 2022. Inventory of glacial curvilineations (GCLs) at the southern periphery of the last Scandinavian Ice Sheet. Geomorphology 400. https://doi.org/10.1016/j.geomorph.2021.108094

Alexander, J., Cooker, M.J., 2016. Moving boulders in flash floods and estimating flow conditions using boulders in ancient deposits. Sedimentology 63, 1582–1595.

Alexander, J., Bridge, J.S., Cheel, R.J., Leclair, S.F., 2001. Bedforms and associated sedimentary structures formed under supercritical water flows over aggrading sand beds. Sedimentology 48, 133–152. https://doi.org/10.1046/j.1365-3091.2001.00357.x

Alley R. B., Lawson D. E., Evenson E. B., Larson G. J. 2003a, Sediment, glaciohydraulic supercooling, and fast glacier flow. Annals of Glaciology 36, 135-141.

Are, F., 1983. Thermal abrasion of coasts. In: Proceedings of the Fourth International Conference on Permafrost, Alaska. National Academy Press, Washington, pp. 24–28.

Arnold, L.J., Bailey, R.M., Tucker, G.E., 2007. Statistical treatment of fluvial dose distributions from southern Colorado arroyo deposits. Quaternary Geochronology 2, 162–167. doi:10.1016/j.quageo.2006.05.003

Baker, V.R., 1973. Paleohydrology and sedimentology of the Lake Missoula flooding in eastern Washington. Geol. Soc. Am. Spec. Pap. 144, 1–79.

Baker, V.R., 1978. Large-scale erosional and depositional features of the Channeled Scabland. In: Baker, V.R., Nummedal, D. (Eds.), The Channeled Scabland. National Aeronautics and Space Administration, pp. 81–115.

Baker, V.R., 2009. The channeled scabland: A retrospective. Annual Review of Earth and Planetary Sciences 37, 393–411. doi:10.1146/annurev.earth.061008.134726

Benito, G., 1997. Energy expenditure and geomorphic work of the cataclysmic Missoula flooding in the Columbia River Gorge, USA. Earth Surf. Process. Landf. 22, 457–472.

Benn, D.I., Owen, L.A., Finkel, R.C., Clemmens, S., 2006. Pleistocene lake outburst floods and fan formation along the eastern Sierra Nevada, California: Implications for the interpretation of intermontane lacustrine records. Quaternary Science Reviews 25, 2729–2748.

Ber, A., 1974. Czwartorzęd Pojezierza Suwalskiego. Biul. Państwowego Inst. Geol. 269, 23–106.

Ber, A., 1982. Marginal zones and deglaciation during the north-polish glaciation in the Suwałki-Augustów Lakeland. Biul. Inst. Geol. 342, 71–89.

Ber, A., 2000. Plejstocen Polski północno-wschodniej w nawiązaniu do głębszego podłoża i obszarów sąsiednich. Pr. Państw. Inst. Geol. 170, 5–89.

Björnsson, H., 1998. Hydrological characteristics of the drainage system beneath a surging glacier. Nature 395, 771–774.

Blair, T.C., 2001. Outburst-flood sedimentation on the proglacial Tuttle Canyon alluvial fan, Owens Valley, California, U.S.A. Journal of Sedimentary Research 71, 657–679.

Blair, T.C., 2002. Alluvial-fan sedimentation from a glacial out- burst flood, Lone Pine, California, and contrasts with meteorological flood fans. In: Martini, I.P., Baker, V.R., Garzon, G. (Eds.), Flood and megaflood processes and deposits, Recent and ancient examples. International Association of Sedimentologists Special Publication 32, 113–140.

Blauvelt, D.J., Russell, A.J., Large, A.R.G., Tweed, F.S., Hiemstra, J.F., Kulessa, B., Evans, D.J.A., Waller R.I., 2020. Controls on jökulhlaup-transported buried ice melt-out at Skeiðarársandur, Iceland: Implications for the evolution of ice-marginal environments. Geomorphology 360, 107–164.

Blott, S.J., Pye, K., 2001. GRADISTAT: a grain size distribution and statistics package for the analysis of unconsolidated sediments. Earth Surf. Process. Landforms 26, 1237–1248. https://doi.org/10.1002/esp.261

Bogacki, M., 1976. Współczesne sandry na przedpolu Skeiðarárjökull (Islandia) i plejstoceńskie sandry w Polsce północno-wschodniej. Rozprawy Uniwersytetu Warszawskiego 99, p. 165.

Bogacki, M., 1980. Types of outwash forms in North-East Poland. Geogr. Polon. 43, 25–34.

Bøtter-Jensen, L., Thomsen, K.J., Jain, M., 2010. Review of optically stimulated luminescence (OSL) instrumental developments for retrospective dosimetry. Radiation Measurements 45, 253–257. doi:10.1016/j.radmeas.2009.11.030

Bridge, J.S., 1993. The interaction between channel geometry, water flow, sediment transport and deposition in braided rivers. In: Best J.L., Bristow C.S. (Eds.), Braided Rivers. Geol. Soc. London Spec. Publ. 75, 13–71.

Carling, P.A., Hoffmann, M., Blatter, A.A., Dittrich, A., 2002. Drag of emergent and submerged rectangular obstacles in turbulent flow above bedrock surface. In: Schleiss, A.J., Bollaert, E. (Eds.), Rock Scour due to Falling High-velocity Jets. Swets and Zeitlinger, Lisse, pp. 83–94.

Carling, P.A., Burr, D.M., Johnsen, T.F., Brennand, T.A., 2009a. A review of open-channel megaflood depositional landforms on Earth and Mars, in: Megaflooding on Earth and Mars. Cambridge University Press, pp. 33–49.

Carling, P.A., Herget, J., Lanz, J.K., Richardson, K., Pacifici, A., 2009b. Channel-scale erosional bedforms in bedrock and in loose granular material: character, processes and implications. In Burr, D. M., Carling, P. A. & Baker, V.R. (Eds.), Megaflooding on Earth and Mars, Cambridge University Press, Cambridge, pp. 13–32.

Carling, P.A., Villanueva, I., Herget, J., Wright, N., Borodavko, P., Morvan, H., 2010. Unsteady 1-D and 2-D hydraulic models with ice-dam break for Quaternary megaflood, Altai Mountains, southern Siberia. Glob. Planet. Change 70, 24–34.

Carling, P.A., 1984. Deposition of fine and coarse sand in an open-work gravel bed (siltation). Canadian Journal of Fisheries and Aquatic Sciences 41, 263–270. doi:10.1139/f84-030

Carling, P.A., 1990. Particle over-passing on depth- limited gravel bars. Sedimentology 37, 345–355.

Carling, P.A., 2013. Freshwater megaflood sedimentation: What can we learn about generic processes? Earth-Science Rev. 125, 87–113. https://doi.org/10.1016/j.earscirev.2013.06.002

Carrivick, J.L., Rushmer, E.L., 2006. Understanding high-magnitude outburst floods. Geol. Today 22, 60–65. https://doi.org/10.1111/j.1365-2451.2006.00554.x

Carrivick, J.L., Russell, A.J., Tweed, F.S., 2004. Geomorphological evidence for jökulhlaups from Kverkfjöll volcano, Iceland. Geomorphology 63, 81–102.

Cartigny, M.J.B., Postma, G., Van den Berg, J.H., Mastbergen, D.R., 2011. A comparative study of sediment waves and cyclic steps based on geometries, internal structures and numerical modelling. Mar. Geol. 280, 40–56.

Cartigny, M.J.B., Ventra, D., Postma, G., van Den Berg, J.H., 2014. Morphodynamics and sedimentary structures of bedforms under supercritical-flow conditions: New insights from flume experiments. Sedimentology 61, 712–748. doi:10.1111/sed.12076

Clayton, L., Attig, J.W., Mickelson, D.M., 1999. Tunnel channels formed in Wisconsin during the last glaciation. In Mickelson, D.M. and J.W. Attig, eds. Glacial processes: past and present. Boulder, CO, Geological Society of America Special Paper 337, 69–82.

Clarke, G., Leverington, D., Teller, J., and Dyke, A., 2004. Paleohydraulics of the last outburst fl ood from glacial Lake Agassiz and the 8200 BP cold event: Quaternary Science Reviews 23, 389–407.

Cofaigh, Ó.C., Evans, D.J.A., Hiemstra, J.F., 2011. Formation of a stratified subglacial 'till' assemblage by ice-marginal thrusting and glacier overriding. Boreas 40, 1–14. 10.1111/j.1502-3885.2010.00177.x.

Costa, J.E., 1984. Physical geomorphology of debris flows. In: Costa, J.E., Fleisher, P.J. (Eds.), Developments and Applications of Geomorphology. Springer-Verlag, Berlin.

Craig, R.G., 1987. Dynamics of a Missoula flood. In: Mayer, L.B., Nash, D. (Eds.), Catastrophic flooding. Binghamton Symposia in Geomorphology, International Series 18, pp. 305–332.

Cronin, S.J., Neall, V.E., Lecointre, J.A., Palmer, A.S., 1999. Dynamic interactions between lahars and stream flow: a case study from Ruapehu volcano, New Zealand. Geological Society of America Bulletin 111, 28–39.

Culter, P.M., P.M. Colgan, Mickelson, D.M., 2002. Sedimentologic evidence for outburst floods from the Laurentide Ice Sheet margin in Wisconsin, USA: implications for tunnel-channel formation. Quat. Int. 90, 23–40.

Duller, R.A., Mountney, N.I.P., Russell, A.J., Cassidy, N.C., 2008. Architectural analysis of a volcaniclastic jo southern Iceland: sedimentary evidence for supercritical flow. Sedimentology 55, 939–964. https://doi.org/10.1111/j.1365-3091.2007.00931.x

Durcan, J.A., King, G.E., Duller, G.A.T., 2015. DRAC: Dose Rate and Age Calculator for trapped charge dating. Quaternary Geochronology 28, 54–61. doi:10.1016/j.quageo.2015.03.012

Dzierżek, J., Zreda, M., 2007. Timing and style of deglaciation of northeastern Poland from cosmogenic 36Cl dating of glacial and glaciofluvial deposits. Geol. Quaterly 51, 203–216.

Elfström, A., 1987. Large catastrophic boulder deposits and catastrophic floods. Geogr. Ann. 69A, 101–121.

Evans, D.J.A., Thomson, S.A., 2010. Glacial sediments and landforms of Holderness, eastern England: A glacial depositional model for the North Sea Lobe of the British–Irish Ice Sheet. Earth-Science Reviews 101, 147–189.

Fay, H., 2002. The formation of ice-block obstacle marks during the November 1996 glacier outburst flood (jökulhlaup), Skeiðarársandur, southern Iceland. In: Martini, I.P., Baker, V.R., Garzon, G. (Eds.), Flood and Megaflood Deposits: Recent and Ancient. Intern. Assoc. Sediment. Spec. Publ. 32, pp. 85–97.

Fielding, C.R., 2006. Upper flow regime sheets, lenses and scour fills: Extending the range of architectural elements for fluvial sediment bodies. Sediment. Geol. 190, 227–240. https://doi.org/10.1016/j.sedgeo.2006.05.009

Fleisher, P.J., Bailey, P.K., Natel, E.M., Russell, A.J., 2010. Subglacial hydraulic scouring and deposition during surge-related outburst floods, Bering Glacier, Alaska. Quaternary Science Reviews 29, 2261–2270. doi:10.1016/j.quascirev.2010.05.027.

Friedman, G.M., Sanders, J.E., 1978. Principles of Sedimentology. Wiley, New York.

Girard, F., Ghienne, J.F., Rubino, J., 2012. Occurrence of hyperpycnal flow sand hybrid event beds related to glacial outburst events in a Late Ordovician proglacial delta (Murzuk Basin, SW Libya). Journal of Sedimentary Research 82, 688–708.

Gomez, B., Smith, L.C., Magilligan, F.J., Mertes, F.A.K. & Smith, N.D., 2000. Glacier outburst floods and outwash plain development: Skeiðdarársandur, Iceland. Terra Nova 12, 126–131.

Gomez, B., Russell, A.J., Smith, L.C., Knudsen, Ó., 2002. Erosion and deposition in the proglacial zone: the 1996 jökulhlaup on Skeiðarársandur, southeast Iceland. In: Snorasson, Á., Finsdóttir, H.P., Moss, M. (Eds.), The extremes of the extremes: extraordinary floods. International Association of Hydrological Sciences Special Publication 271, 217–221

Gruszka, B., van Loon A.j. 2011. Genesis of a giant gravity-induced depression (gravifossum) in the Enköping esker, S. Sweden. Sedimentary Geology 235, 304–313.

Hansen, L., Tassis, G., Høgaas, F., 2020. Sand dunes and valley fills from Preboreal glacial-lake outburst floods in south- eastern Norway - beyond the aeolian paradigm. Sedimentology 67, 810–848. https://doi.org/10.1111/sed.12663

Hanson, M.A., Clague, J.J., 2016. Record of glacial Lake Missoula floods in glacial Lake Columbia, Washington. Quaternary Science Reviews 133, 62–76.

Harrison, D., Ross, N., Russell, A.J., Jones, S.J., 2022. Ground-penetrating radar (GPR) investigations ofa large-scale buried ice-marginal landsystem, Skeiðararsandur, SE Iceland. Boreas 51, 824–846 https://doi. org/10.1111/bor.12587

Harrison, D., Ross, N., Russell, A.J., Jones, S.J., 2023. Geophysical reconstruction of the late Holocene proximal proglacial landsystem at Skeiðarársandur, southeast Iceland. Journal of Quaternary Science 38, 947–969.

Hart, J.K., Boulton, G.S., 1991. The interrelationship between glaciotectonic deformation and glaciodeposition. Quaternary Science Reviews 10, 335–350.

Hermanowski, P. Piotrowski, J.A., 2023. Origin of glacial curvilineations by subglacial meltwater erosion: evidence from the Stargard drumlin field, Poland. Earth Surface Processes and Landforms 48, 231–486.

Hiscott, R.N., Middleton, G.V., 1980. Fabric of coarse deep-water sandstones Tourelle Formation, Quebec, Canada. J. Sediment. Petrol. 50, 703–722.

Høgaas, F., Longva, O., 2016. Mega deposits and erosive features related to the glacial lake Nedre Glomsjø outburst flood, southeastern Norway. Quaternary Science Reviews 151, 273–291. https://doi:10.1016/j.quascirev.2016.09.015

Hornung, J.J., Asprion, U., Winsemann, J., 2007. Jet-efflux deposits of a subaqueous ice-contact fan, glacial Lake Rinteln, northwestern Germany. Sedimentary Geology 193, 167–192. https://doi:10.1016/j.sedgeo.2005.11.024

Ito, M., Ishikawa, K., Nishida, N., 2014. Distinctive erosional and depositional structures formed at a canyon mouth: a lower Pleistocene deep-water succession in the Kazusa forearc basin on the Kazusa forearc basin on the Boso Peninsula, Japan. Sedimentology 61, 2042–2062.

Jol, H.M. (Ed.), 2008. Ground Penetrating Radar Theory and Applications. Elsevier, Amsterdam.

Jørgensen, F., Sandersen, P.B.E., 2006. Buried and open tunnel valleys in Denmark – erosion beneath multiple ice sheets. Quaternary Science Reviews 25, 1339–1363.

Kavanaugh, J.L., Clarke, G.K.C., 2000. Evidence for extreme pressure pulses in the subglacial water system. J. Glaciol. 46, 206–212.

Kehew, A.E., Lord, M.L., 1986. Origin and large-scale erosional features of glacial-lake spillways in the northern Great Plains. Geological Society of America Bulletin 97, 162–177.

Kehew, A.E., Teller, J.T., 1994. History of late glacial runoff along the southwestern margin of the Laurentide Ice Sheet. Quaternary Science Reviews 13, 859–877.

Kehew, A.E., Lord, M.L., Kozlowski, A.L., Fisher, T.G., 2009. Proglacial megaflooding along the margins of the Laurentide Ice Sheet. In: Burr, D., Carling, P.A., Baker, V.R. (Eds.), Megaflooding on earth and Mars. Cambridge University Press, 104–127.

Kehew, A.E., Piotrowski, J.A., Jørgensen, F., 2012. Tunnel valleys: Concepts and controversies – a review. Earth-Science Reviews, 113(1–2), 33– 58. https://doi.org/10.1016/j.earscirev.2012.02.002

Kehew, A.E., 1993. Glacial-lake outburst erosion of the GrandValley, Michigan and impacts on glacial lakes in the Lake Michigan basin. Quaternary Research 239, 36–44.

Kehew, A.E., Teller, J.T., 1994. Glacial-lake spillway incision and deposition of a coarse-grained fan near Waterous, Saskatchewan. Canadian Journal of Earth Science 31, 544–553.

Kjær, K., Sultana, L., Krqgerb, J., Schomackera, A., 2004. Architecture and sedimentation of outwash fans in front of the Mýrdalsjfkull ice cap, Iceland. Sedimentary Geology 172, 139–163.

Kirkham James D. Kirkham, Kelly A. Hogan, Robert D. Larter, Neil S. Arnold, Jeremy C. Ely, Chris D. Clark, Ed Self, Ken Games, Mads Huuse, Margaret A. Stewart, Dag Ottesen, Julian A. Dowdeswell, J.A., Tunnel valley formation beneath deglaciating mid-latitude ice sheets: Observations and modelling. Quaternary Science Reviews 323, 107680.

Komar, P. D., 1983. Shapes of streamlined islands on Earth and Mars: Experiments and analyses of the minimum-drag form. Geology 11, 651–654.

Komar, P. D., 1984. The lemniscate loop - Comparisons with the shapes of streamlined landforms: Journal of Geology 92 (2), 133–146.

Kondracki, J., Pietkiewicz, S., 1967. Czwartorzęd północno-wschodniej Polski. In: Galon, R., Dylik, J. (Eds.), Czwartorzęd Polski. Wyd. Nauk. PWN, Warszawa, pp. 207–258.

Kostic, S., Sequeiros, O., Spinewine, B., Parker, G., 2010. Cyclic steps: A phenomenon of supercritical shallow flow from the high mountains to the bottom of the ocean. Journal of Hydro-environment Research 3(4), 167–172.

Kostic, S., Casalbore, D., Chiocci, F., Lang, J., Winsemann J., 2019. Role of upper-flow-regime bedforms emplaced by sediment gravity flows in the evolution of deltas. J. Mar. Sci. Eng. 7, 5. doi:10.3390/jmse7010005

Kozlowski, A.L., Kehew, A.E., Bird B.C., 2005. Outburst flood origin of the Central Kalamazoo River Valley, Michigan, USA. Quarterly Science Reviews, 24(22), 2354–2374.

Krüger, J., Kjær, K.H., 1999. A data chart for field description and genetic interpretation of glacial diamicts and associated sediments - with examples from Greenland, Iceland, and Denmark. Boreas 28, 386–402. https://doi:10.1111/j.1502-3885.1999.tb00228.x

Krzyszkowski, D., 2002. Sedimentary successions in ice-marginal fans of the Late Saalian glaciation, southwestern Poland, Sedimentary Geology 149, 93–109. https://doi.org/10.1016/S0037-0738(01)00246-9.

Krzyszkowski, D., Zieliński, T., 2002. The Pleistocene end moraine fans: controls on their sedimentation and location. Sedimentary Geology 149, 73–92.

Lang, J., Alho, P., Kasvi, E., Goseberg, N., Winsemann, J., 2019. Impact of Middle Pleistocene (Saalian) glacial lake-outburst floods on the meltwater-drainage pathways in northern central Europe: insights from 2D numerical flood simulation. Quaternary Science Reviews 209, 82–99.

Lang, J., Brandes, C., Winsemann, J. 2017a. Erosion and deposition by supercritical density flows during channel avulsion and backfilling: Field examples from coarse-grained deepwater channel-levée complexes (Sandino Forearc Basin, southern Central America). Sedimentary Geology 349, 79–102. https://doi.org/10.1016/j.sedgeo.2017.01.002

Lang, J., Le Heron, D.P., Van den Berg, J.H., Winsemann, J., 2021. Bedforms and sedimentary structures related to supercritical flows in glacigenic settings. Sedimentology 68, 1539–1579. https://doi.org/10.1111/sed.12776

Lang, J., Sievers, J., Loewer, M., Igel, J., Winsemann, J., 2017b. 3D architecture of cyclic-step and antidune deposits in glacigenic subaqueous fan and delta settings: Integrating outcrop and ground-penetrating radar data. Sedimentary Geology 362, 83–100. https://doi:10.1016/j.sedgeo.2017.10.011

Lang, J., Winsemann, J., 2013. Lateral and vertical facies relationships of bedforms deposited by aggrading supercritical flows: From cyclic steps to humpback dunes. Sedimentary Geology 296, 36–54. https://doi.org/10.1016/j.sedgeo.2013.08.005

Larson, G.J., Daniel, E., Lawson, D.E., Evenson, E.B., Alley, R.B., Knudsen, Ó., Lachniet, M.S., Goetz, S.L., 2006. Glaciohydraulic supercooling in former ice sheets? Geomorphology 75, 20–32.

Lekkala, M.R., Latheef, M., Jung, J.H., Coraddu, A., Zhu, H., Srinil, N., Lee, B.-H., Kim, D.K., 2022. Recent advances in understanding the flow over bluff bodies with different geometries at moderate Reynolds numbers. Ocean Engineering 261, 111611. https://doi.org/10.1016/j.oceaneng.2022.111611

Lesemann, J-E., Piotrowski, J.A., Wysota, W., 2010. „Glacial curvilineations": New glacial landforms produced by longitudinal vortices in subglacial meltwater flows. Geomorphology 120, 153–161.

Lesemann, J-E., Piotrowski, J.A., Wysota, W., 2014. Genesis of the 'glacial curvilineation' landscape by meltwater processes under the former Scandinavian Ice Sheet, Poland. Sedimentary Geology 312, 1–18.

Lord. M.L., Kehew, A.E., 1987. Sedimentology and paleohydrology of glacial-lake outburst deposits in southeastern Saskatchewan and northwestern North Dakota. Geological Society of America Bulletin 99, 663–673.

Lowe, D.R., 1982. Sediment gravity flows II: deposition models with special references to the deposits of high-density turbidity currents. Journal of Sedimentary Petrology 52, 279–297.

Lunt I.A., Bridge, J.S., 2007. Formation and preservation of open-framework gravel strata in unidirectional flow. Sedimentology 54, 71–87. https://doi: 10.1111/j.1365-3091.2006.00829.x

Maizels, J.K., 1991. Origin and evolution of Holocene sandurs in areas of jökulhlaup drainage, south Iceland. In: Maizels, J.K., Caseldine, C. (Eds.), Environmental Change in Iceland. Past and Present, Kluwer, pp. 267–300.

Maizels, J., 1993. Lithofacies variations within sandur deposits: the role of runoff regime, flow dynamics and sediment supply characteristics. Sedimentary Geology 85, 299–325.

Maizels, J.K., 1995. Sediments and landforms of modern proglacial terrestrial enviroments. In: Menzies, J. (Ed.), Modern Glacial Environments; Processes, dynamics and sediments. Butterworth-Heinemann, Oxford, pp. 365–416.

Maizels, J., 1997. Jokulhlaup deposits in proglacial areas. Quaternary Science Reviews 16, 793–819. https://doi.org/10.1016/S0277-3791(97)00023-1

Malde, H.E., 1968. The catastrophic Late Pleistocene Bonneville Flood in the Snake River Plain, Idaho. US Geological Survey Professional Paper 596, p. 52.

Marren, P.M., 2002. Criteria for identifying high magnitude flood events in the proglacial fluvial sedimentary record. In: Snorrason, Á., Finnsdóttir, H.P., Moss, M. (Eds.), The Extremes of the Extremes: Extraordinary Floods: IAHS Publication, 271, pp. 237–241.

Marren, P.M., Schuh, M., 2009. Criteria for identifying jökulhlaup deposits in the sedimentary record. Chapter 12. In: Burr, D.M., Carling, P.A., Baker, V.R. (Eds.), Megaflooding on Earth & Mars. Cambridge University Press, Cambridge, pp. 225–242.

Marren, P.M., Russell, A.J., Knudsen, Ó., 2002. Discharge magnitude and frequency as a control on proglacial fluvial sedimentary systems. In: Dyer, F., Thoms, M.C., Olley, J.M. (Eds.), Structure, Function and Management Implications of Fluvial Sedimentary Systems, 276. IAHS Publication, pp. 297–303.

Meinsen, J., Winsemann, J., Weitkamp, A., Landmeyer, N., Lenz, A., Dölling, M., 2011. Middle Pleistocene (Saalian) lake outburst floods in the Münsterland Embayment (NW Germany): Impacts and magnitudes. Quaternary Science Reviews 30, 2597–2625. https://doi:10.1016/j.quascirev.2011.05.014

Miall, A.D., 1978. Lithofacies types and vertical profile models in braided river deposits: a summary. Fluv. Sedimentology 5, 597–600.

Miall, A.D., 2006. The geology of fluvial deposits. Sedimentary facies, basin analysis, and petroleum geology. Springer. Berlin, Heidelberg, New York.

Murray, A.S., Marten, R., Johnston, A., Martin, P., 1987. Analysis for naturally occurring radionuclides at environmental concentrations by gamma spectrometry. Journal of Radioanalytical and Nuclear Chemistry 115, 263–288.

Muto, T., Yamagishi, C., Sekiguchi, T., Yokokawa, M., Parker, G., 2012. The hydraulic autogenesis of distinct cyclicity in delta foreset bedding: flume experiments. Journal of Sedimentary Research 82, 545–558. https://doi.org/10.2110/jsr.2012.49

Nemec, W., Muszyński, A., 1982. Volcaniclastic alluvial aprons in Tertiary of Sophia District (Bulgaria). Annales Societas Geologorum Polaniae 52, 239–303.

Neuman, C.M., Sanderson, S., Sutton, S., 2013. Vortex shedding and morphodynamic response of bed surfaces containing non-erodible roughness elements. Geomorphology 198, 45–56.

O'Connor, J.E., 1993. Hydrology, hydraulics, and geomorphology of the Bonneville Flood. Geological Society of America, Special Paper 274, p. 83.

Paterson, W.S.B., 1994. The Physics of Glaciers. Butterworth-Heinemann, p. 496.

Peters, J.L., Brennand, T.A., 2020. Palaeogeographical reconstruction and hydrology of glacial Lake Purcell during MIS 2 and its potential impact on the Channelled Scabland, USA. Boreas 49, 461–476. https://doi:10.1111/bor.12434

Pierson, T.C., Scott, K.M., 1985. Downstream dilution of a lahar: Transition from debris flow to hyperconcentrated streamflow. Water Resources Research 21, 1511-1524.

Piotrowski, J.A., Tulaczyk, S. 1999. Subglacial conditions under the last ice sheet in northwest Germany: ice-bed separation and enhanced basal sliding? Quaternary Science Reviews 18, 737–751.

Piotrowski, J.A., 1994. Tunnel valley formation in north-west Germany: geology, mechanisms of formation and subglacial bed conditions for the Bornhoved tunnel valley. Sed. Geol. 89, 107–141.

Postma, G., Cartigny, M.J.B. and Kleverlaan, K., 2009. Structureless, coarse-tail graded Bouma Ta formed by internal hydraulic jump of the turbidity current? Sedimentary Geology 219, 1–6.

Postma, G., Kleverlaan, K., Cartigny, M.J.B., 2014. Recognition of cyclic steps in sandy and gravelly turbidite sequences, and consequences for the Bouma facies model. Sedimentology 61, 2268–2290.

Postma, G., Nemec, W., Kleinspehn, K.L., 1988. Large floating clasts in turbidites: a mechanism for their emplacement. Sedimentary Geology 58, 47–61.

Randriamazaoro, R., Dupeyrat, L., Costard, F. and Gailhardis, E.C., 2007. Fluvial thermal erosion: heat balance integral method. Earth Surface Processes and Landforms 32, 1828–1840.

Rinterknecht, V., Marks, L., Piotrowski, J., Raisbeck, G., Yiou, F., Brook, E., Clark, P., 2005. Cosmogenic 10Be ages on the Pomeranian Moraine, Poland. Boreas 34, 186–191. https://doi.org/10.1080/03009480510012926

Rinterknecht, V.R., Bitinas, A., Clark, P.U., Raisbeck, G.M., Yiou, F., Brook, E.J., 2008. Timing of the last deglaciation in Lithuania. Boreas 37, 426–433. https://doi.org/10.1111/j.1502-3885.2008.00027.x

Rinterknecht, V.R., Clark, P.U., Raisbeck, G.M., Yiou, F., Bitinas, A., Brook, E.J., Marks, L., Zelčs, V., Lunkka, J.P., Pavlovskaya, I.E., Piotrowski, J.A., Raukas, A., 2006. The last deglaciation of the southeastern sector of the Scandinavian ice sheet. Science 311, 1449–1452. https://doi.org/10.1126/science.1120702

Roberts, M.J., Russell, A.J., Tweed, F.S., Knudsen, Ó., 2000a. Rapid sediment entrainment and englacial deposition during jökulhlaups. Journal of Glaciology 153, 349–351.

Roberts, M.J., Russell, A.J., Tweed, F.S., Knudsen, Ó., 2000b. Ice fracturing during jökulhlaups: implications for englacial floodwater routing and outlet development. Earth Surface Processes and Landforms 25, 1429–1446.

Roberts, M.J., Russell, A.J., Tweed, F.S., Knudsen, Ó., 2001. Controls on englacial sediment deposition during the November 1996 jökulhlaup, Skeiðarárjökull, Iceland. Earth Surface Processes and Landforms 26, 935–952.

Røe, S.-L., 1987. Cross-strata and bedforms of probable transitional dune to upper-stage plane-bed origin from a Late Precambrian fluvial sandstone, northern Norway. Sedimentology 34, 89–101.Rushmer, E.L., 2006. Sedimentological and geomorphological impacts of the jökulhlaup (glacial outburst flood) in January 2002 at Kverkfjöll, northern Iceland. Geogr. Ann. A 88, 43–53. https://doi.org/10.1111/j.0435-3676.2006.00282.x

Rushmer, E.L., Russell A.J., Tweed, F.S., Knudsen Ó., Marren, P.M., 2002. The role of hydrograph shape in controlling glacier outburst flood (jökulhlaup) sedimentation. IAHS Publ. 276, 305–313.

Russell, A.J., 1992. Geomorphological Effects of Jökulhlaups, West Greenland. (PhD thesis) University of Aberdeen, Aberdeen.

Russell, A.J., 1993. Obstacle marks produced by flow around stranded ice blocks during a glacier outburst flood (jökulhlaup) in west Greenland. Sedimentology 40, 1091–1111.

Russell, A.J., 2007. Controls on the sedimentology of an ice-contact jökulhlaup-dominated delta, Kangerlussuaq, west Greenland. Sedimentary Geology 193, 131–148.

Russell, A.J., 2009. Jökulhlaup (ice-dammed lake outburst flood) impact within a valley-confined sandur subject to backwater conditions, Kangerlussuaq, West Greenland. Sedimentary Geology 215, 33–49. https://doi.org/10.1016/j.sedgeo.2008.06.011

Russell, A.J., Knudsen, Ó., 1990. Controls on the sedimentology of the November 1996 jökulhlaup deposits, Skeiðarársandur, Iceland. In: Smith, N.D., Rogers, J. (Eds.), Fluvial Sedimentology VI,. IAS Special Publication 28, 315–329.

Russell, A.J., Knudsen, Ó., 1999. An ice-contact rhythmite (turbidite) succession deposited during the November 1996 catastrophic outburst flood (jökulhlaup), Skeiðarárjökull, Iceland. Sedimentary Geology 127, 1–10.

Russell, A.J., Knudsen, Ó., 2002a. Jökulhlaup deposits at the Ásbyrgi Canyon, northern Iceland: sedimentology and implications for flow type. In: Snorasson, A., Finnsdóttir, H.P., Moss, M. (Eds.), The Extreme of the Extremes: Extraordinary Floods. Proceedings Symposium at Reykjavik, Iceland, July 2000, 271. IAHS Publication, 107–112.

Russell, A.J., Knudsen, O., 2002b. The effects of glacier outburst flood flow dynamics on ice-contact deposits: November 1996 jökulhlaup, Skeiðarársandur, Iceland. In:Martini, I.P., Baker, V.R., Garcon, G. (Eds.), Flood and Megaflood Processes and Deposits: Recent and Ancient Examples, Special Publication 32 of the IAS. Blackwell Science, Oxford, 17–35.

Russell, H.A.J., Arnott, R.W.C., 2003. Hydraulic-jump and hyperconcentrated-flow deposits of a glacigenic subaqueous fan: oak ridges moraine, southern Ontario, Canada. J. Sediment. Res. 73, 887–905.

Russell, A.J., Marren, P.M., 1999. Proglacial fluvial sedimentary sequences in Greenland and Iceland: a case study from active proglacial environments subject to jokulhlaups. In: Jones, A.P., Tucker, M.E., Hart, J.K. (Eds.), The Description and Analysis of Quaternary Stratigraphic Field Sections. Technical Guide. Quaternary Research Association, London, pp. 171–208.

Russell, A.J., Tweed, F.S., Knudsen, Ó ., 2000. Flash flood at Sólheimajökull heralds the reawakening of an Icelandic subglacial volcano. Geol. Today, 103–107.

Russell, A.J., Knudsen, Ó., Fay, H., Marren, P.M., Heinz, J., Tronicke, J., 2001. Morphology and sedimentology of a giant supraglacial, ice-walled, jökulhlaup channel, Skeiðarársandur, Iceland. Glob. Planet. Change 28, 203–226.

Russell, A.J., Tweed, F.S., Harris, T., 2003. High-energy sedimentation, Creag Aoil, Spean Bridge, Scotland: Implications for meltwater movement and storage during Loch Lomond Stadial (Younger Dryas) ice retreat. Journal of Quaternary Science 18, 415–430. https://doi:10.1002/jqs.761

Russell, A.J., Fay, H., Marren, P.M., Tweed, F.S., Knudsen Ó., 2005. Icelandic jökulhlaup impacts. In: Caseldine, C.J., Russell, A.J., Knudsen, Ó., Harðardóttir, H. (Eds.), Iceland: Modern Processes and Past Environments. Developments in Quaternary Science 5, 154–203.

Russell, A.J., Roberts, M.J., Fay, H., Marren, P.M., Cassidy, N.J., Tweed, F.S., Harris, T., 2006. Icelandic jökulhlaup impacts: Implications for ice-sheet hydrology, sediment transfer and geomorphology. Geomorphology 75, 33–64. https://doi.org/10.1016/j.geomorph.2005.05.018

Russell, A.J., Gregory, A.G., Large, A.R.G., Fleisher, P.J., Harris, T., 2007. Tunnel channel formation during the November 1996 jökulhlaup, Skeiðarárjökull, Iceland. Annals of Glaciology 45, 95–103.

Russell, A.J., Tweed, F., Roberts, M., Harris, T., Gudmundsson, M., Knudsen, O., Marren, P., 2010. An unusual jökulhlaup resulting from subglacial volcanism, Sólheimajökull, Iceland. Quat. Sci. Rev. 29: 1363–1381.

Rychel, J., Sokołowski, R.J., Sieradz, D., Hrynowiecka, A., Mirosław-Grabowska, J., Sienkiewicz, E., Niska, M., Szymanek, M., Zbucki, Ł., Ciołko, U., Rogóż-Matyszczak, A., 2023. Late Pleniglacial-Late Glacial climate oscillations detected in the organic lacustrine succession at the Lipowo site, north-eastern Poland. J. Quat. Sci. 38, 186–207. https://doi.org/10.1002/jqs.3477

Sallenger, A.H., 1979. Inverse grading and hydraulic equivalence in grain-flow deposits. Journal of Sedimentary Petrology 49, 553–562.

Schillaci, C., Braun, A., Kropácek, J., 2015. Terrain Analysis and Landform Recognition, in: Clarke, L.E., Nield, J.M. (Eds.), Geomorphological Techniques (Online Edition). British Society for Geomorphology, London, UK Chapter 2.4.2.

Schlömer, O., Grams, P.E., Buscombe, D., Herget, J., 2021. Geometry of obstacle marks at instream boulders - integration of laboratory investigations and field observations. Earth Surface Processes and Landforms 46, 659-679.

Shakesby, R.A., 1985. Geomorphological effects of jökulhlaups and ice-dammed lakes, Jotunheimen, Norway. Nor. Geogr. Tidsskr. 39, 1–16.

Shaw, J., Gorrell, G., 1991. Subglacial formed dunes with bimodal and graded gravel in the Trenton drumlin field, Ontario. Géographie Physique Quaternaire 45, 21–34.

Shaw, J., Munro-Stasiuk, M., Sawyer, B., Beaney, C., Lesemann, J.-E., Musacchio, A., Rains, B., Young, R.R., 1999. The channeled scabland: back to Bretz? Geology 27, 605–608.

Shoemaker, E.M., 1992. Water sheet outburst floods from the Laurentide ice sheet. Can. J. Earth Sci. 29, 1250–1264.

Slootman, A., Cartigny, M.J.B., 2020. Cyclic steps: Review and aggradation-based classification. Earth-Science Rev. 201. https://doi.org/10.1016/j.earscirev.2019.102949

Smith, G.A., 1993. Missoula flood dynamics and magnitudes inferred from sedimentology of slack-water deposits on the Columbia Plateau, Washington. Geol. Soc. Am. Bull. 105, 77–100.

Sobota, I., Weckwerth, P., Nowak, M., 2016. Surge dynamics of Aavatsmarkbreen, Svalbard, inferred from the geomorphological record. Boreas 45, 360–376.

Sobota, I., Weckwerth, P., Grajewski, T., Dziembowki M., Greń, K., Nowak, M., 2018. Short-term changes in thickness and temperature of the active layer in summer in the Kaffioyra region, NW Spitsbergen, Svalbard. Catena 160, 141–153.

Strong, N., Paola, C., 2008. Valleys that never were: time versus stratigraphic surfaces. J. Sediment. Res. 78, 579–593.

Sutton, S.L.F., Neuman, C.M., 2008. Variation in bed level shear stress on surfaces sheltered by nonerodible roughness elements. Journal of Geophysical Research, 113(F3). https://doi.org/10.1029/2007jf000967;

Tylmann, K., 2014. Dynamika procesów glacjalnych na obszarze Garbu Lubawskiego podczas ostatniego zlodowacenia. PhD Thesis. UMK, Toruń.

van der Wateren, F.M., 1999. Structural geology and sedimentology of the Heiligen- hafen till section, northern Germany. Quaternary Science Reviews 18, 1625–1640.

Waller, R.I., van Dijkt, A.G.P., Knudsen Ó., 2001; Jökulhlaup-related ice fracture and supraglacial water release during the November 1996 jökulhlaup, Skeiðarárjökull, Iceland. Geografiska Annaler 83A, 29–38.

Weckwerth, P., Greń, K., Sobota, I., 2019. Controls on downstream variation in surficial sediment size of an outwash braidplain developed under high Arctic conditions updates (Kaffioyra, Svalbard). Sedimentary Geology 387, 75–86.

Weckwerth, P., Kalińska, E., Wysota, W., Krawiec, A., Adamczyk, A., Chabowski, M., 2022. What does transverse furrow train in scabland-like topography originate from? The unique records of upper-flow-regime bedforms of a glacial lake-outburst flood in NE Poland. Quaternary International 617, 40–58.

Weckwerth, P., Pisarska-Jamroży, M., 2014. Periglacial and fluvial factors controlling the sedimentation of Pleistocene breccia in NW Poland. Geografiska Annaler, A, Physical Geography, 415–430.

Weckwerth, P., Sobota, I., Greń, K., 2021. Where will widening occur in an outwash braidplain? A new approach to detecting controls on fluvial lateral erosion in a glacierized catchment (north-western Spitsbergen, Svalbard). Earth Surface Processes and Landforms 46(5), 942–967.

Weckwerth, P., Wysota, W., 2024. Unique landscape originated by cataclysmic glacial floods at the Weichselian glaciation decline in north-eastern Poland. In: Migoń P. (Ed.), Landscapes and Landforms of Poland, pp. 655–675.

Weckwerth, P., Wysota, W., Piotrowski, J.A., Adamczyk, A., Krawiec, A., Dąbrowski, M., 2019. Late Weichselian glacier outburst floods in North-Eastern Poland: Landform evidence and palaeohydraulic significance. Earth-Science Rev. 194, 216–233. https://doi.org/10.1016/j.earscirev.2019.05.006

Wells, G.H., Dugmore, A.J., Beach, T., Baynes, E.R.C., Sæmundsson, Þ., Luzzadder-Beach, S., 2022. Reconstructing glacial outburst floods (jökulhlaups) from geomorphology: Challenges, solutions, and an enhanced interpretive framework. Prog. Phys. Geogr. 46, 398–421. https://doi.org/10.1177/03091333211065001

Wentworth, C.K., 1922, A scale of grade and class terms for clastic sediments: The Journal of Geology 30 (5), 377–392.

Winsemann, J., Alho, P., Laamanen, L., Goseberg, N., Lang, J., Klostermann, J., 2016. Flow dynamics, sedimentation and erosion of glacial lake outburst floods along the Middle Pleistocene Scandinavian Ice Sheet (northern central Europe). Boreas 45, 260–283. https://doi.org/10.1111/bor.12146

Winsemann, J., Hornung, J.J., Meinsen, J., Asprion, U., Polom, U., Brandes, C., Bußmann, M., Weber, C., 2009. Anatomy of a subaqueous ice-contact fan and delta complex, Middle Pleistocene, north-west Germany. Sedimentology 56, 1041–1076. https://doi.org/10.1111/j.1365-3091.2008.01018.x

Winsemann, J., Brandes, C., Polom, U., 2011. Response of a proglacial delta to rapid high-amplitude lake level change: an integration of outcrop data and high resolution shear wave seismic. Basin Research 23, 22–52. https://doi.org/10.1111/j.1365-2117.2010.00465.x

Winsemann, J., Lang, J., Polom, U., Loewer, M., Igel, J., Pollok, L., Brandes, C., 2018. Ice-marginal forced regressive deltas in glacial lake basins: geomorphology, facies variability and large-scale depositional architecture. Boreas 47, 973–1002. https://doi.org/10.1111/bor.12317

Wysota, W., Weckwerth, P., Adamczyk, A., Piotrowski, J.A., Sokólska, A., 2020. Morphology and origin of glacial curvilineations (GCLs) east of Hańcza Lake, Suwałki Lakeland. In: Weckwerth, P., Wysota, W., Kalińska, E. (Eds.), Glacial megaflood landforms and sediments in North-Eastern Poland. Wyd. Nauk. UMK, Toruń, pp. 61–69.

Zieliński, T., Van Loon, A.J., 2000. Subaerial terminoglacial fans III: overview of sedimentary characteristics and depositional model. Geologie en Mijnbouw 79, 93–107.

Zieliński, T., Van Loon, A.J., 2003. Pleistocene sandur deposits represent braidplains, not alluvial fans. Boreas 32, 590–612. doi 10.1080/03009480310004170

Zieliński, T., 1989. Lithofacies and palaeoenvironmental characteristics of Suwałki outwash (Pleistocene, Northwest Poland). Ann Soc Geol Polon 59, 249–270.

Zieliński, T., 1993. Sandry Polski północno-wschodniej – osady i warunki sedymentacji. Uniw Śląski, Katowice, 96.

Figure captions:

Fig. 1. A – morphology and regional units of the study area in north-eastern Poland (after Solon et al., 2018); B – landforms origin in the Megaflood Landform System (after Weckwerth et al., 2019, modified); C – simplified model of sedimentary environment showing the major elements of Megaflood Landform System in submarginal and proglacial settings; D – morphology of marginal zone with the floodwater outlets (gates, ice portals) and outburst fans near Bachanowo and Szeszupka; E – geomorphological map of the southern part of the Szeszupa Tunnel Valley and marginal zone associated with the Bachanowo and Szeszupka Outburst Fans development.

Fig. 2. A and B – morphology of the Bachanowo and Szeszupka Outburst Fans; C and D – GLOF-related features in proximal part of the Western Spillway and at the submarginal position (white arrows – local directions of proglacial floodwater outflow; for legend see Fig. 1).

Fig. 3. Longitudinal cross profiles showing morphology of the BOF (A) and SOF (B) and landforms developed at submarginal position.

Fig. 4. A – landscape morphology of the BOF apex and ice-front position during the GLOF; B – landforms origin in the area of the Bachanowo Gate (for legend see Fig. 1); C – streamlined residual hummocks separated by distributive channels in the proximal zone of the BOF; D – sediments forming the residual hummock in the Bachanowo 2 site (site location in panels A and B, and in Fig. 2C).

Fig. 5. Morphology of small-scale bedforms originated from GLOFs in the areas of analysed key sites at submarginal position (B1 – Bachanowo 1 site) and in proximal and distal zones of the BOF and SOF. The genetic types of bedforms were distinguished on the basis of their morphology, location and spatial relationships, considering the sedimentary

successions recognised in the key sites. (B2-4 - Bachanowo 2-4 sites; S1-2 - Szeszupka 1-2 sites) (iGCL - initial GCL ridges; rh - residual hummocks; eb - erosional bars; pb - pendant bars; sc - scours; sct - scour trains; ch - channels; cb - chute bars; kh - kettle holes).

Fig. 6. Sedimentary succession in the Bachanowo 1 site (1-10 – deformed sediments in unit U3: 1 – massive well-sorted gravels with openwork texture and boulder lags in the bottom part, 2 – clast-supported massive boulders and gravels with sandy matrix forming the gravifossum bottom, 3 – fine-grained sands with ripple cross-lamination or horizontally stratified deformed by shear folds and reverse or normal microfaults; 4 – crude stratified sands with admixture of gravels deformed by reverse faults, 5 – fine-grained sands and silts forming diapir-like structure deformed due to lateral pressure exerted by the weight of the slumped till clasts (8), 6 – massive gravels and sands in the upper part of diapir-like structure, 7 – horizontally laminated fine-grained sands and silts deformed by reverse microfaults at the contact with till clasts, 8 – large-scale clasts of diamicton (till); 9 – massive sands with gravels with crude stratification or gravels with openwork texture, deformed by normal faults and folds; ruc – rip-up clasts; mss1 and mss2 – major slip surfaces 1 and 2; ds – diapir-like structure; hs – horst structure; gf – gravifossum).

Fig. 7. Radargrams A-A’ and B-B’ and their interpretation: A – radar profile across proximal zone of the BOF (for location see Fig. 4B); B – radar profile across distal zone of the BOF (for location see Fig. 5C) (1 – radar facies RF1: low amplitude, sparse, chaotic and incoherent reflections, 2 – radar facies RF2: low amplitude, planar or wavy reflections, 3 – radar facies RF3: continuous and planar reflections, 4 – radar facies RF4: strong, continuous and finely dense undulated reflections, 5 – radar facies RF5: very high amplitude, wavy and continuous reflections, 6 – radar facies RF6: low amplitude and locally noisy reflections, 7 – radar facies RF7: low and moderate, continuous reflections).

Fig. 8. Sediments of isolated scour in the Bachanowo 4 site (site location in Figs 2C and 5D): A and B – lithofacies associations 1-3 recognised in profiles 1 and 2 at the Bachanowo 4 site (red circles – OSL samples and their lab numbers); C – upper member of the first scour infill sedimentary succession capped by gravelly lag of the second scour infill; D – crude concave-up cross-stratification with openwork texture as a main sediment body of the scour infill; E – second and complete scour infill sedimentary succession (GBm→GRsc/GPsc(o)→DGm(m_2)/GSm→SFm/SFr); F – low-angle and sinusoidal cross-stratified granules with openwork texture interpreted as sediments of upstream migrating antidunes.

Fig. 9. Sediments deposited in the zone of scour train in the Szeszupka 1 site (site location in Figs 2D and 5E): A – scour train morphology and the Szeszupka 1 site location; B – scour train morphology and presumed sedimentary successions related with flow stages; C and D – lithofacies associations 1–4 recognised in profiles 1 and 2 at the Szeszupka 1 site; E and F – concentric and concave-up gravelly scour infills (facies GRsc(o)/GSsc); G - facies association 2 (related with rising flow stage), interpreted as sediments of lateral scours associated with submerged and partly grounded boulder.

Fig. 10. Sedimentary succession of a pendant bar identified in the Szeszupka 2 site: A and B lithofacies associations 1-2 recognised in profiles 1 and 2 at the Szeszupka 2 site; C-E – sedimentary succession Gsc(o)→GSm→Ss/Sh recording scour development associated with the hydraulic jump zone (migrating upstream), located downstream of the elongated ridges infill; F-G – sediments of pendant bar deposited in the near wake under conditions of unstable structure of the secondary flows and abrupt changes in the flow competence.

Fig. 11. Sedimentary successions of small-scale chute bar recognised in the Bachanowo 3 site: A - sedimentary units U1 and U2 separated by erosional contact (red circles – OSL samples and their lab numbers); B - upward coarsening succession of sedimentary rhythm

GSs/Ss, GRh(o) with lower gravelly laminae and upper composed of sands with admixture of granules or granules with openwork texture, deformed by the normal faults; C – the second sedimentary rhythm GRs(o)/SGs comprising sinusoidal stratified granules with openwork texture (lower layer) and sands with admixture of gravels (upper layer); D and E – the third sedimentary rhythm characterised by sheet-like sandy beds dipping downstream and changes in stratification type, from horizontal to sinuous (SGh/Sh→SGs/Ss); F – sedimentary unit U2 with facies association GSm, Sm representing the post-GLOF deposition.

Fig. 12. A and B – spatial and temporal changes in englacial feeding system at submarginal position influencing floodwater outlets and outburst fans development during GLOF1 (A) and their transformation during GLOF2 (B); C – two types of floodwater drainage and linked subglacial morphology as factors controlling the development of different floodwater outlets ($\alpha_{B1\text{-}3}$ and $\alpha_{S1\text{-}3}$ – ice-surface slope for BOF and SOF respectively; $\beta_{B1\text{-}3}$ and $\beta_{S1\text{-}3}$ for BOF and SOF, respectively – adverse subglacial slope; A – coefficient in the ice-sheet surface calculation based on formulas proposed by Paterson (1994) and Piotrowski and Tulaczyk (1999).

Fig. 13. Conceptual model showing the development of various floodwater outlets, associated outburst fans and their small-scale bedforms origin in response to the GLOF stages and changes in the englacial feeding system.

Fig. 14. Spatio-temporal model of small-scale bedforms on the outburst fan surface and two types of floodwater outlets developed in relation with GLOF stages (A) and conceptual illustration of conditions and processes forming small scale bedforms on outburst fan surface (B).

Table captions:

Table 1. Lithofacies codes used for recording the sediments lithology and structure (textural symbols: grain size classes according to the GRADISTAT software (after Blott and Pye, 2001), in brackets sediment classes proposed by Wentworth (1922) (granules and pebbles) and Friedman and Sanders (1978) (cobbles); for lithofacies interpretation see Table 3).

Table 2. Summary of doses, mean and modelled ages, used model, unused MAM2 age, number (n) of accepted and total aliquots, skewness, probability (p), overdispersion (OD), dose rates and water content.

Table 3. Bedforms morphology, sedimentary successions and origin on outburst fan surface at rising and falling stages of the GLOF (bedform morphology: L – length, W – width, D – depth, H – height; statistical parameters for the grain-size distributions: d_{50} – median grain diameter, σ – sorting, Sk – skewness, Kg – kurtosis).

Textural symbols	Sediments		Structural symbols	Stratification
D	Diamicton		m	Massive
B	Medium, large, very large	Boulders	s	Stratified diamicton (in general)
BC	Very small, small (cobbles)		sc	Planar, trough or sigmoidal cross-stratification, , concentric and concave-up laminae across the palaeoflow
GP	Fine, medium, coarse, very coarse (pebbles)	Gravels (G)		
GR	Very fine (granules)		bl	Backset cross-stratification
S	Sands: very fine, fine, medium, coarse, very coarse			
F	Fines: silts and clays		h	Horizontal stratification
Clast/matrix relationship				
m_1	Matrix-supported, clast poor		s	Sinusoidal stratification (for sands and gravels).
			l	Low-angle cross-stratification or subhorizontal stratification
m_2	Matrix-supported, clast moderate		r	Ripple cross-lamination
(o)	Openwork		(d)	Deformed

Key site	Lab ID (Lund-)	Mean dose [Gy]	Mean age [ka]	Modelled age [ka]	Age model	MAM3 age [ka; unused]	n [accepted/total]	Skewness	p	OD	Dose rate [Gy/ka]	Water content [%]
Bachanowo 3	21009	64.0±5.8	28.4±2.8	25.5±2.5	CAM	12.7±1.1	26/39	0.63	0.00	44	2.25±0.09	11
Bachanowo 3	21010	33.1±2.0	13.5±1.0	13.2±0.9	CAM	8.9±0.7	23/27	0.03	0.02	25	2.45±0.10	11
Bachanowo 4	21011	164±9.5	106.6±7.7	102.3±7.8	CAM	57.9±2.8	28/38	0.65	0.01	31	1.54±0.07	11
Bachanowo 4	21012	159.4±14.4	71.7±7.2	64.4±6.3	CAM	29.4±1.7	28/35	0.94	0.01	45	2.22±0.09	11

Table 3 (Editable version)

	Bedforms		Rising stage and/or peak discharge			Waning stage		
Fan zone	Type (site)	Morphology	Sedimentary facies and their successions	textural properties for GLOF sediments: $d_{50}/\sigma/Sk/Kg$ (if available)	Interpretation	Sedimentary facies and their successions	textural properties for GLOF sediments: $d_{50}/\sigma/Sk/Kg$ (if available)	Interpretation
Proximal	Isolated scour (GPR profile A-A')	Oval, isolated and enclosed depressions; L: up to 45 m W: up to 22 m D: up to 2 m	Gravelly lags (radar facies RF4)	-	Bed scouring; formed under fully submerged flow conditions	Stratified and massive sediments (radar facies RF5→RF6)	-	Scour infill
	Residual hummock (Bachanowo 2)	L: 91-422 m W: 37-52 m H: up to 4 m	Pre-GLOF: Dm(m_1), DSm(m_1)(d), DSs(m_1); GLOF: SGm	-	Bed scouring to minimize resistance to flow; formed under fully submerged flow conditions	Pre-GLOF sediments	-	Flow separation and channelization causing channel lateral erosion
Distal	Isolated scour (Bachanowo 4)	L: 43-85 m W: 35-47 m D: up to 2.5 m	GSm/GBm/BCm→GRsc/GPsc(o)	MPS=0.8 m; Matrix in GSm/GBm/BCm: 2.9–6.6/22.1–38.6/-0.5–-1.4/1.6–3.3; GRsc(GPsc)(o): 3–1.6/2.8–21.3/-1.4–1.7/3.3–9.7	Repeated incision related with chute-and-pools development, gravelly lags followed by gravel bedload sheets formation and hyperconcentrated flows; scour infill and rhythmic deposition representing pulses of floodwater outflow or multiple flood events; sediment concentration increasing	DGm(m_2)→GRh/GRl →Sr/SFm/SFr	Matrix in DGm(m_2): 0.1/5.1/-1.3/4.1 GRh/GRl(o): 2.6/23.6/-0.8/2.3 Sr: 0.2/	Scour infilling as a result of massive suspension fall-out, migrating antidunes, humpback dunes and ripples
	Scour train (Szeszupka 1)	three elongated and enclosed depressions, each has: L: 25–52 m W: 18–37 m (L and W increase downstream) D: 1.5–2.5 m; widths of ridges dividing scours: 10-15 m (increase downstream)	GBm→ GRsc/GSsc→Gbl→ SFm/SFh	MPS for GBm=0.22 m; GRsc(o): 2.1–9.5/7.1–49.6/-2–-0.5/1.5-8; SFm/SFh: 0.1/2.5/-0.5/6	Development of cyclic steps as a result of upslope-migrating hydraulic jumps; widespread repeated phases of scouring in the zones of the strong vortices, gravelly lags formation followed by scour infill; high sediment flux	GRsc → Gm/GSm/SGm	GRsc: 2–8.6/7–31/-1.5–-2/3.4–8.1; Martix in Gm/GSm: 0.13/2.1/-1/7.7	Rapid deposition and scour infilling by massive suspension fall-out and matrix-supported and poorly sorted gravel accumulation or hyperconcentrated flows

	Pendant bar (Szeszupka 2)	L: 95-152 m W: 40-53 m H: up to 1.5 m			GRm/GSm/GBm, Sl/Sh→ GSsc/GRsc(o)→SFm/Sm	GRm/GSm/GBm: 1.8–2.5/2.7–3.4/-0.3–-0.9/3.7–4.6; Sl/Sh: 0.48/2/-0.2/5.5; SFm/Sm: 0.04–0.1/4.4–9.3/-0.7–-0.5/2.2–3.6	Deposition in deeper areas downstream of flow obstacles due to flow separation ; submerged flow conditions and abrupt changes in flow competence; formation of gravelly bed sheets, sandy upper plane bed, up-flow migrating antidunes and scours in the zones of hydraulic jumps; intensive outwash of a fine fraction under the condition of a Froude-supercritical flow regime

	Chute bar (Bachanowo 3)	L: 94-167 m
		W: 91-85 m
		H: up to 1.8 m
					Rhythmic bedding and fining-upward succession;
					first phase (rhythm 1): GSm/SGs(GRh(o);
					second phase (rhythm 2): GRs(o)/SGs;
					third phase: SGh/Sh→SGs/Ss
						Rhythm 1: 0.17–0.98/3.9–8.6/-2.1–-1/4.6–7.5
						Rhythm 2: 9.5–0.8/3.8–45.7/-0.3–-0.2/1.3–2.1;
						SGh/Sh: 0.4–0.6/3.2-10.8/0.3–-1.2/
						SGs/Ss: 0.2/2.2/0.04/7.8
							Three-stage vertical accretion limited to the areas of channel widening and/or at the mouth of channels; deposition by repeated flow pulses along with progressively reduction in flow energy; final deposition under the condition of Froude-supercritical flow (upper plane bed and antidunes formation)

	Erosional bar (GPR profile B-B')	L: 70-687 m W: 23-72 m H: up to 2 m			GLOF various sediments	-	Flow channelization, fan surface dissection, channel lateral migration forming surface characterized by uniform gradient

Figure 1 (Color)

Click here to access/download;Figure (Color);Weckwerth et al_Fig_01_corrected.jpg

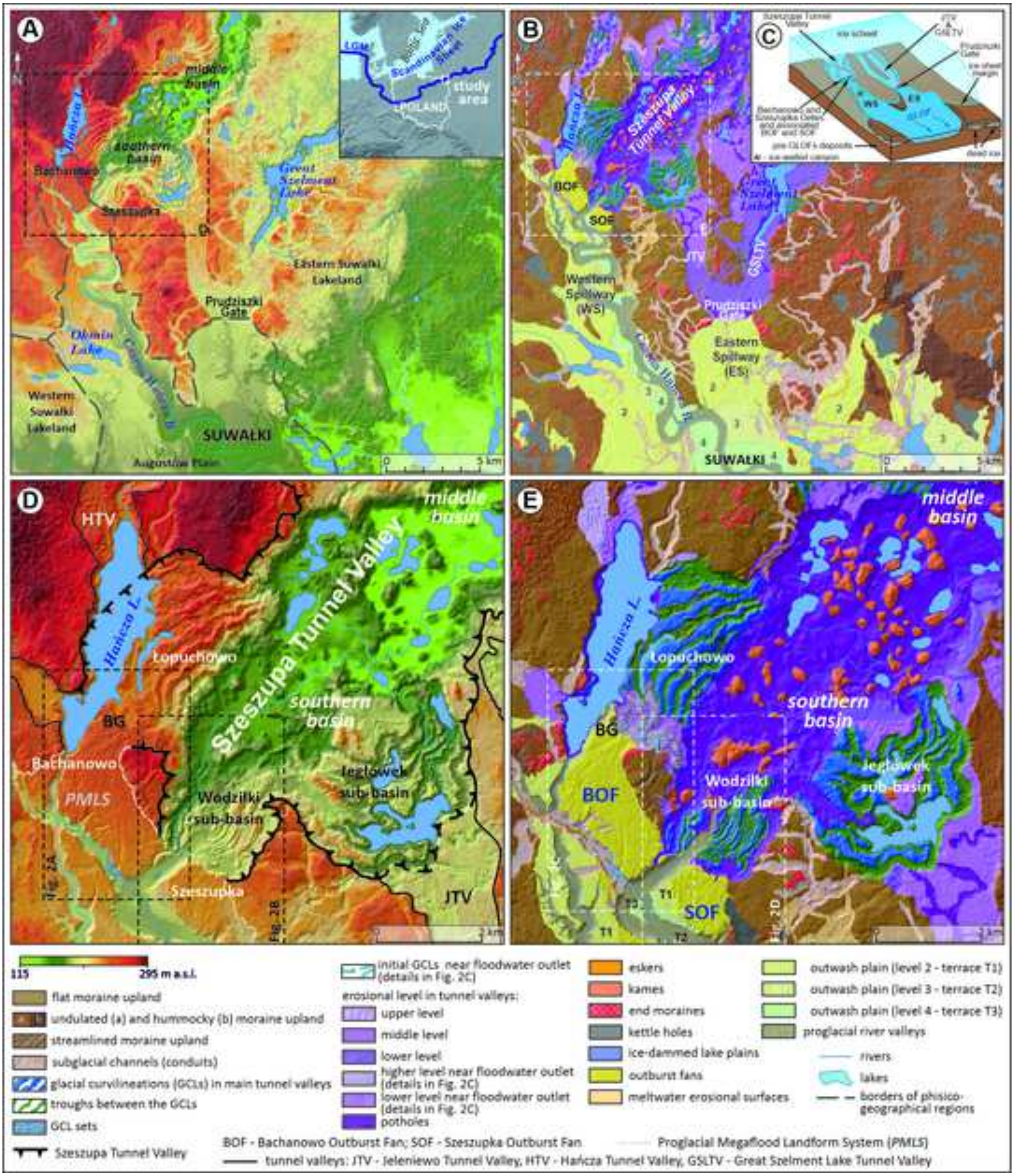

Figure 2

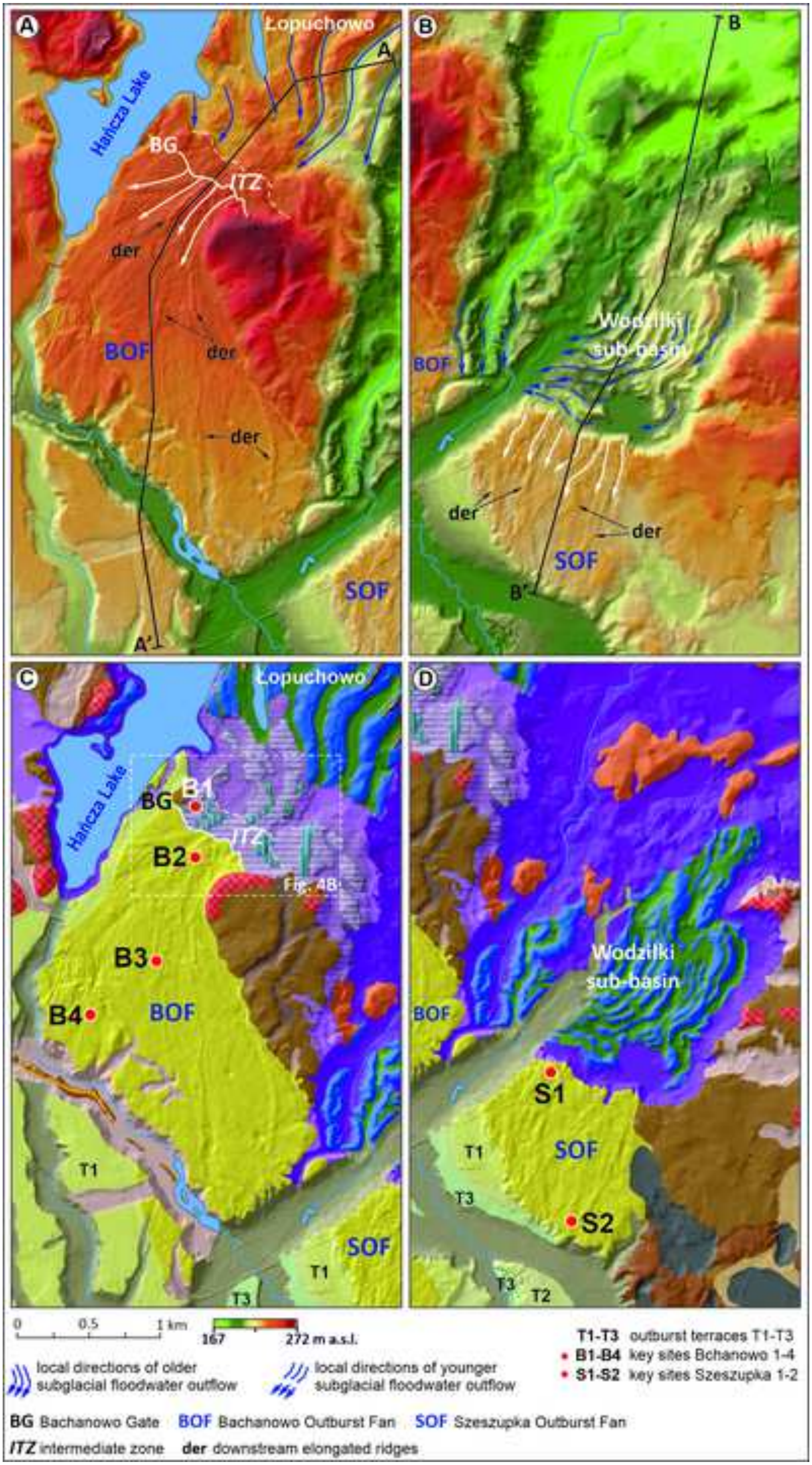
A
Łopuchowo
Hańcza Lake
BG
ITZ
der
BOF
der
der
SOF
A'
B
Wodziłki sub-basin
BOF
der
der
SOF
B'
C
Łopuchowo
Hańcza Lake
BG
B1
ITZ
B2
Fig. 4B
B3
B4
BOF
T1
SOF
T1
T3
D
Wodziłki sub-basin
BOF
S1
T1
SOF
T3
S2
T3
T2
0 0.5 1 km
167 272 m a.s.l.
T1-T3 outburst terraces T1-T3
B1-B4 key sites Bachanowo 1-4
S1-S2 key sites Szeszupka 1-2
local directions of older subglacial floodwater outflow
local directions of younger subglacial floodwater outflow
BG Bachanowo Gate
BOF Bachanowo Outburst Fan
SOF Szeszupka Outburst Fan
ITZ intermediate zone
der downstream elongated ridges

Figure 3 (Color) Click here to access/download;Figure (Color);Weckwerth et al_Fig_03_corrected.jpg

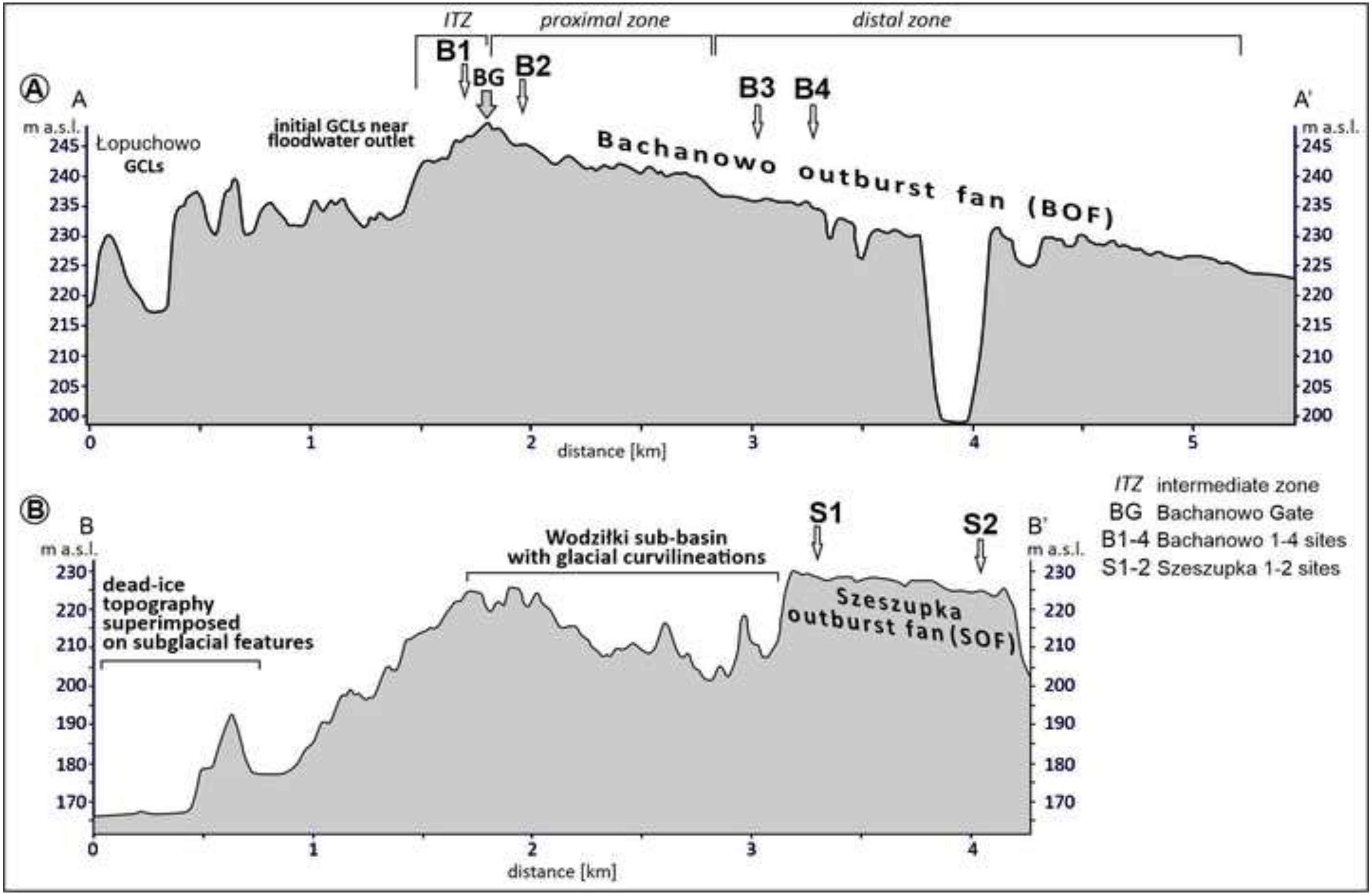

Figure 4

Click here to access/download;Figure (Color);Weckwerth et al_Fig_04.jpg

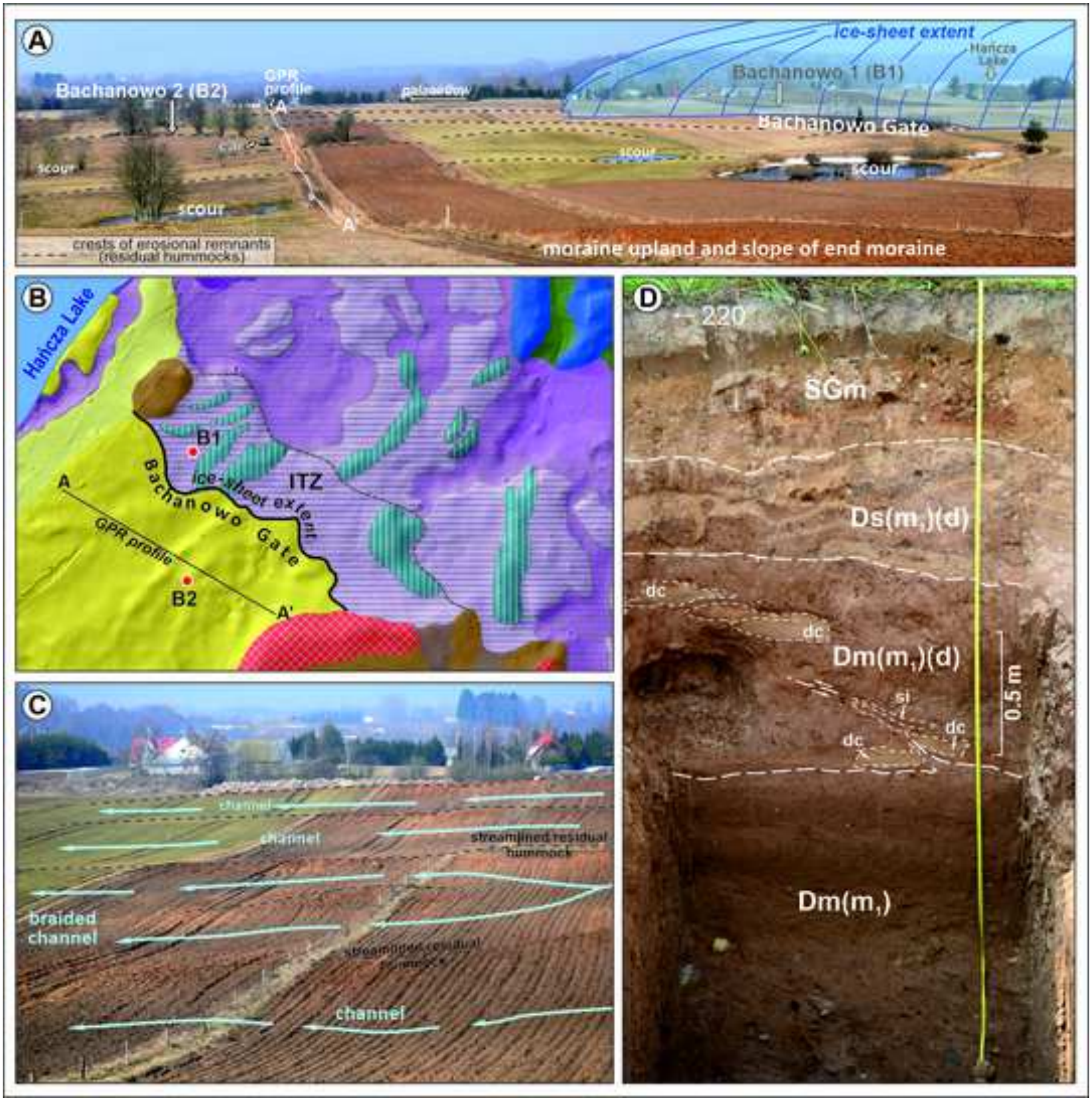

Figure 5 (Color)

Click here to access/download;Figure (Color);Weckwerth et al_Fig_05_corrected.jpg

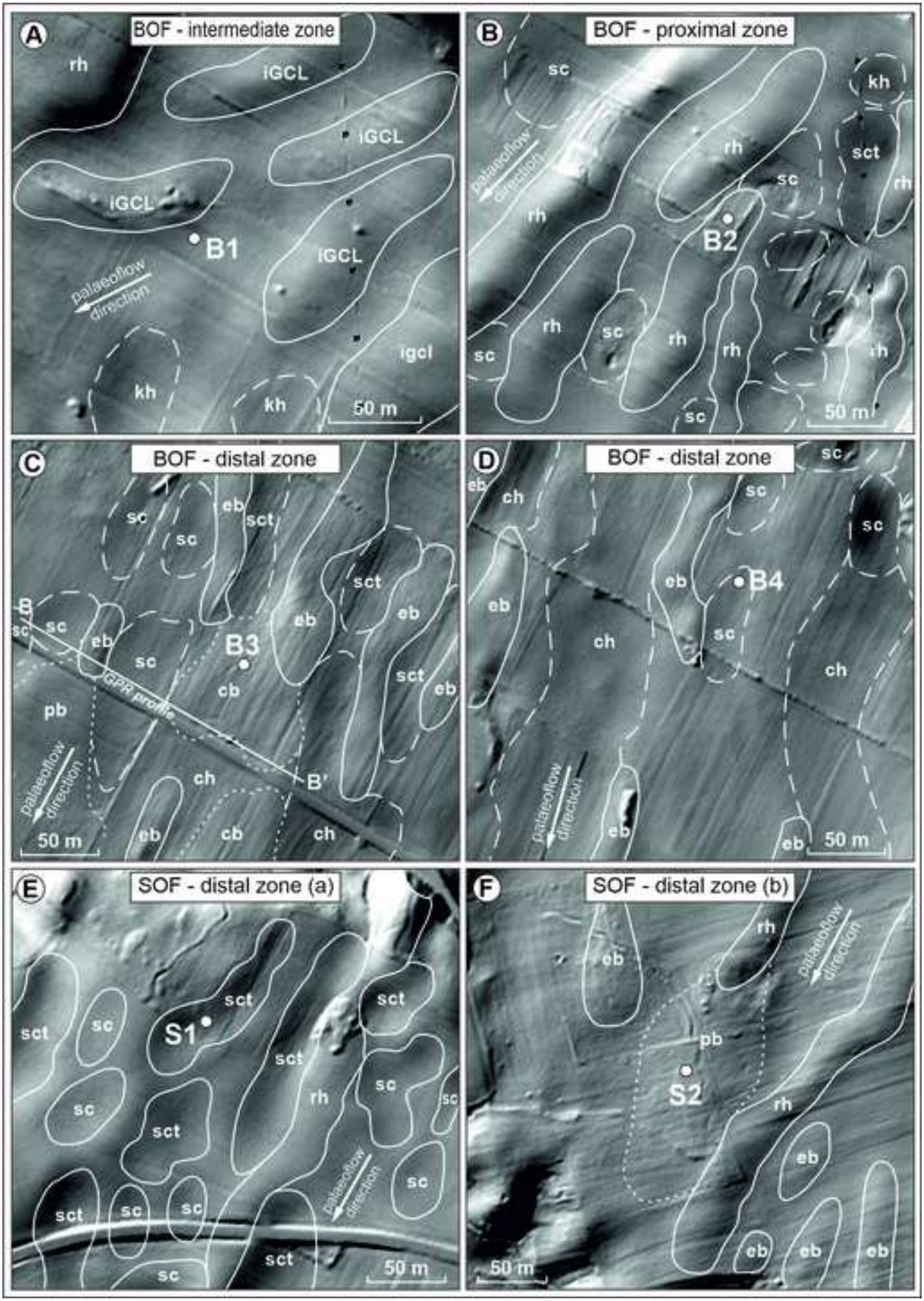

Figure 6 Click here to access/download;Figure (Color);Weckwerth et al_Fig_06.jpg

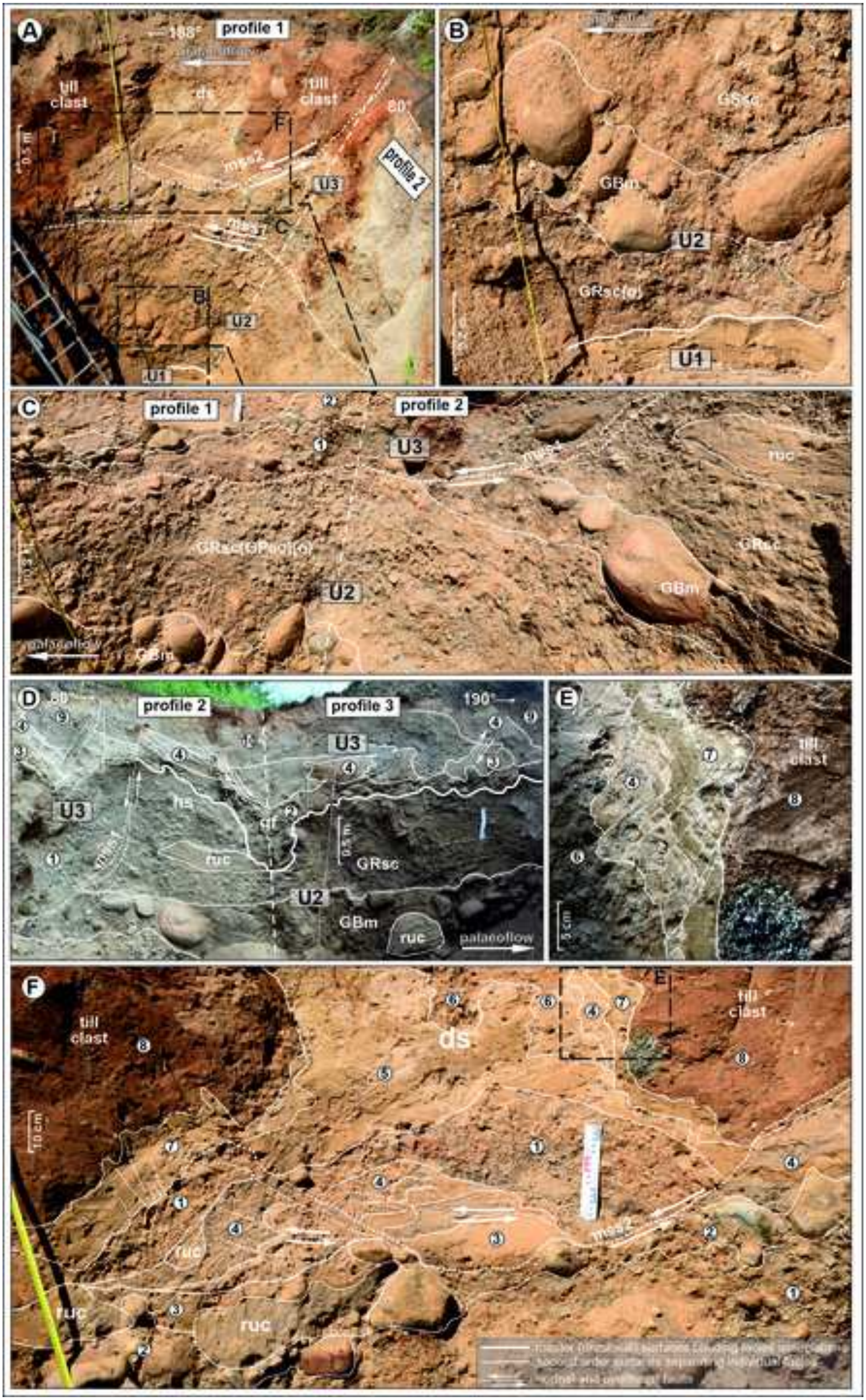

Figure 7

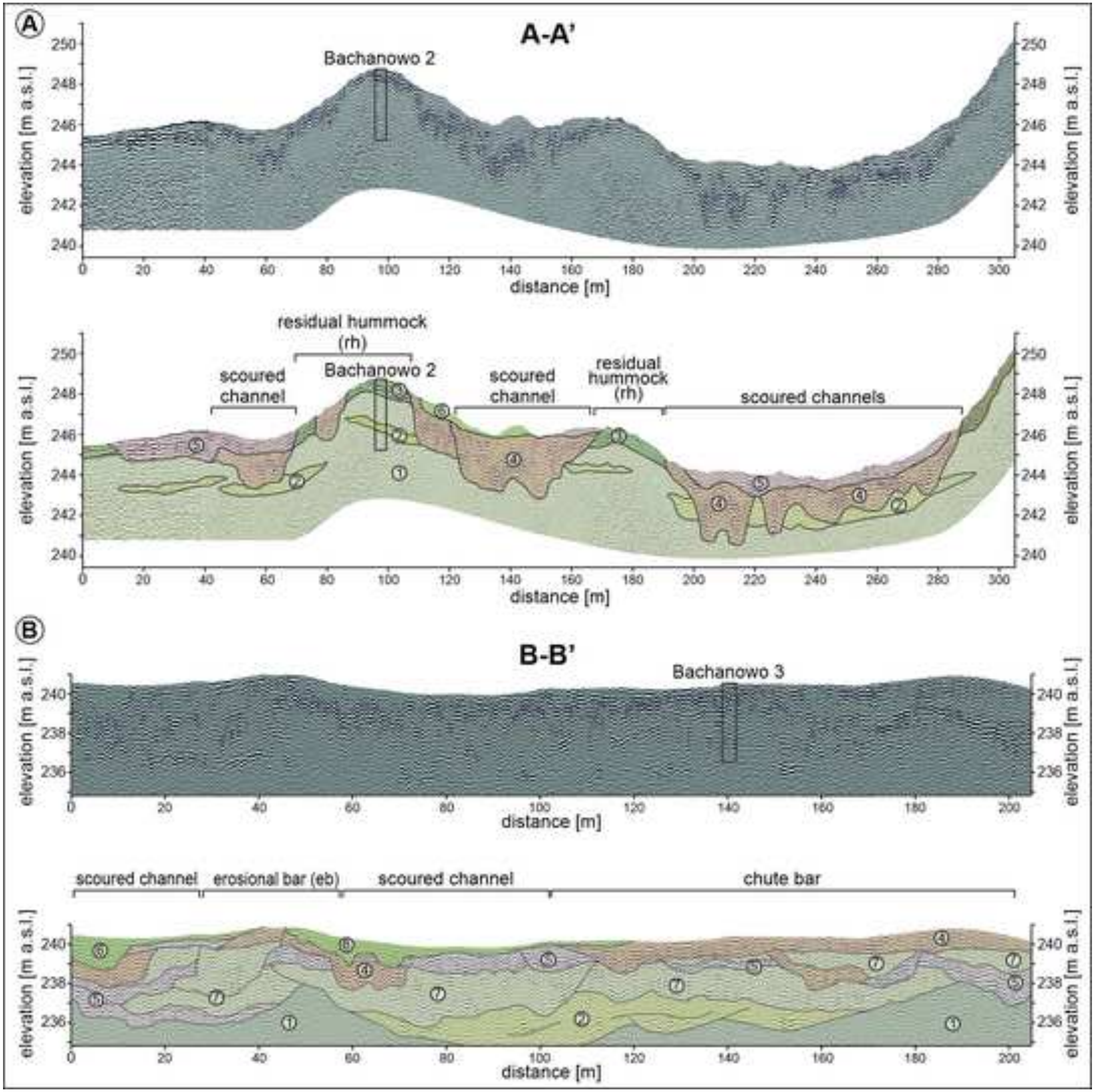
A
A-A'
Bachanowo 2
elevation [m a.s.l.]
distance [m]
residual hummock (rh)
scoured channel
Bachanowo 2
scoured channel
residual hummock (rh)
scoured channels
B
B-B'
Bachanowo 3
scoured channel
erosional bar (eb)
scoured channel
chute bar

Figure 8 (Color)

Click here to access/download;Figure (Color);Weckwerth et al_Fig_08_corrected.jpg

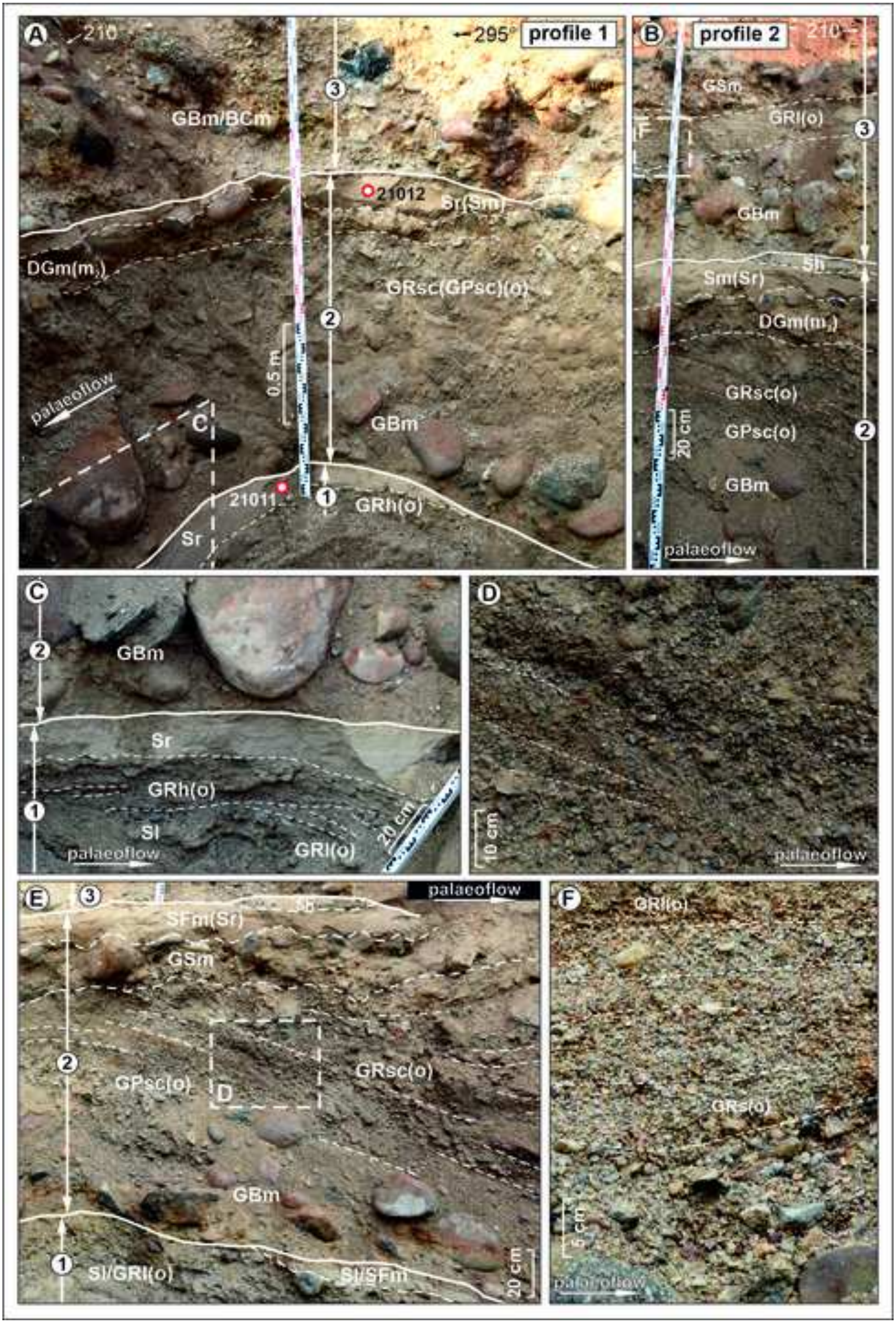

Figure 9 (Color)

Click here to access/download;Figure (Color);Weckwerth et al_Fig_09_corrected.jpg

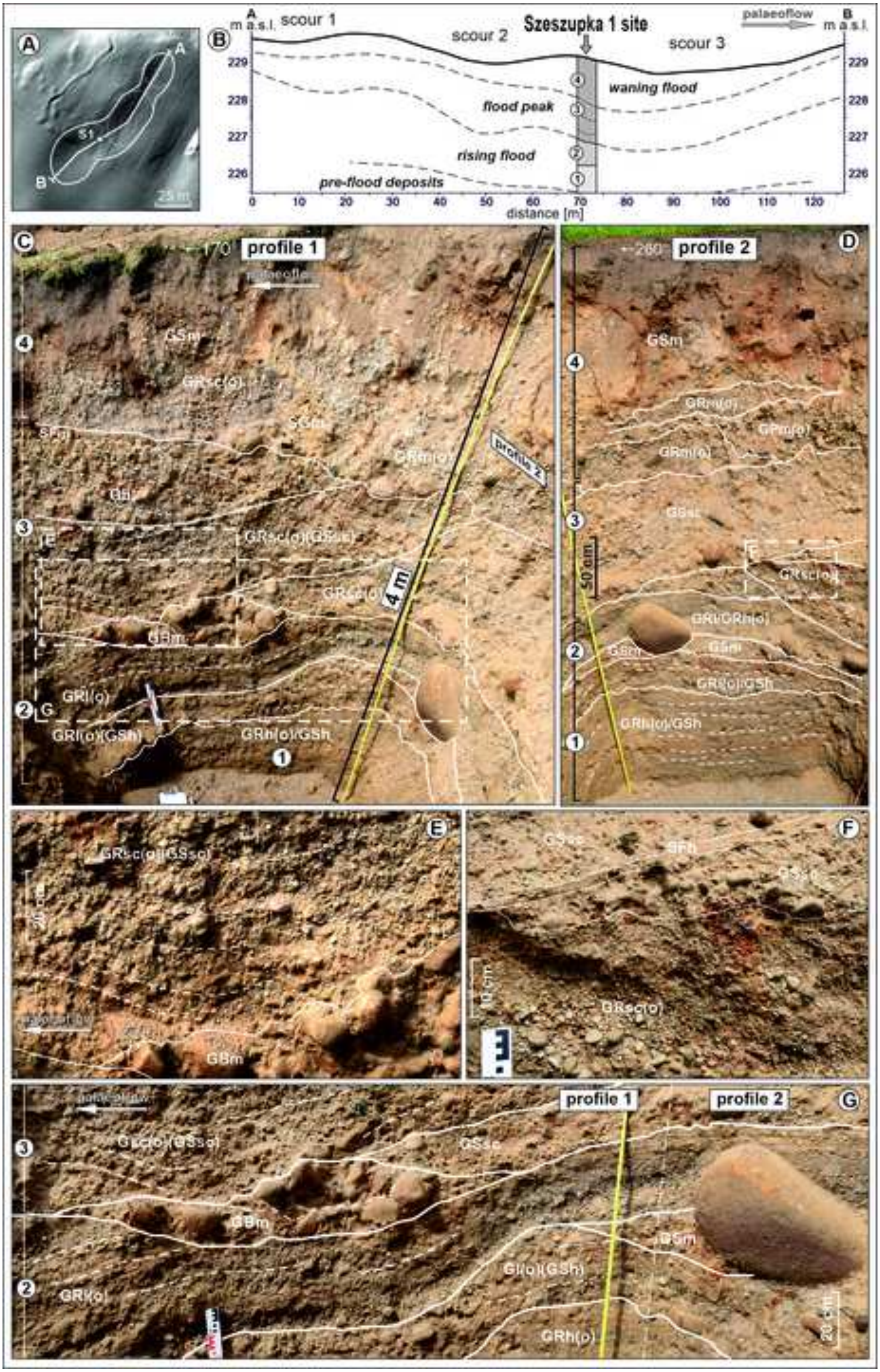

Figure 10

Click here to access/download;Figure (Color);Weckwerth et al_Fig_10.jpg

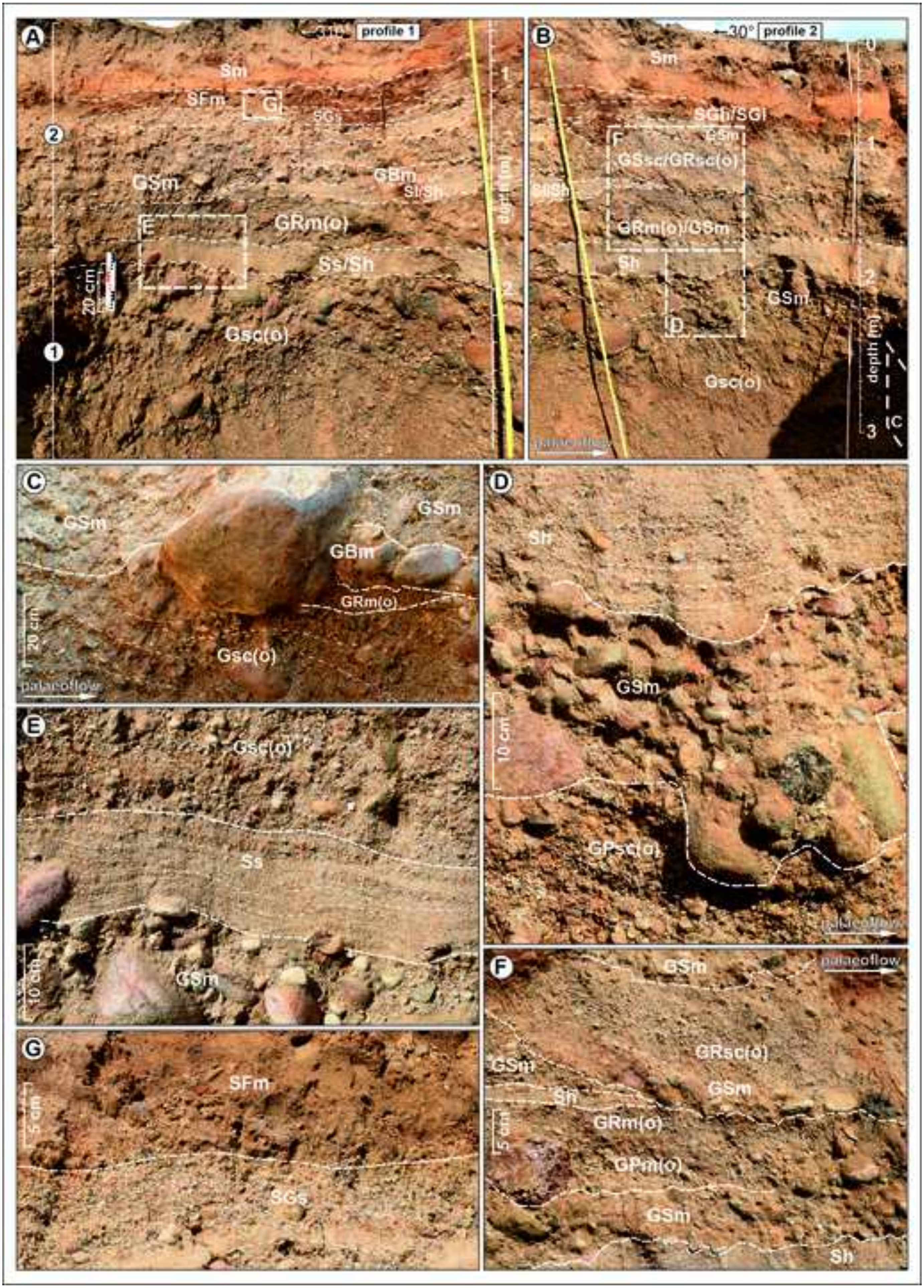

Figure 11 (Color)

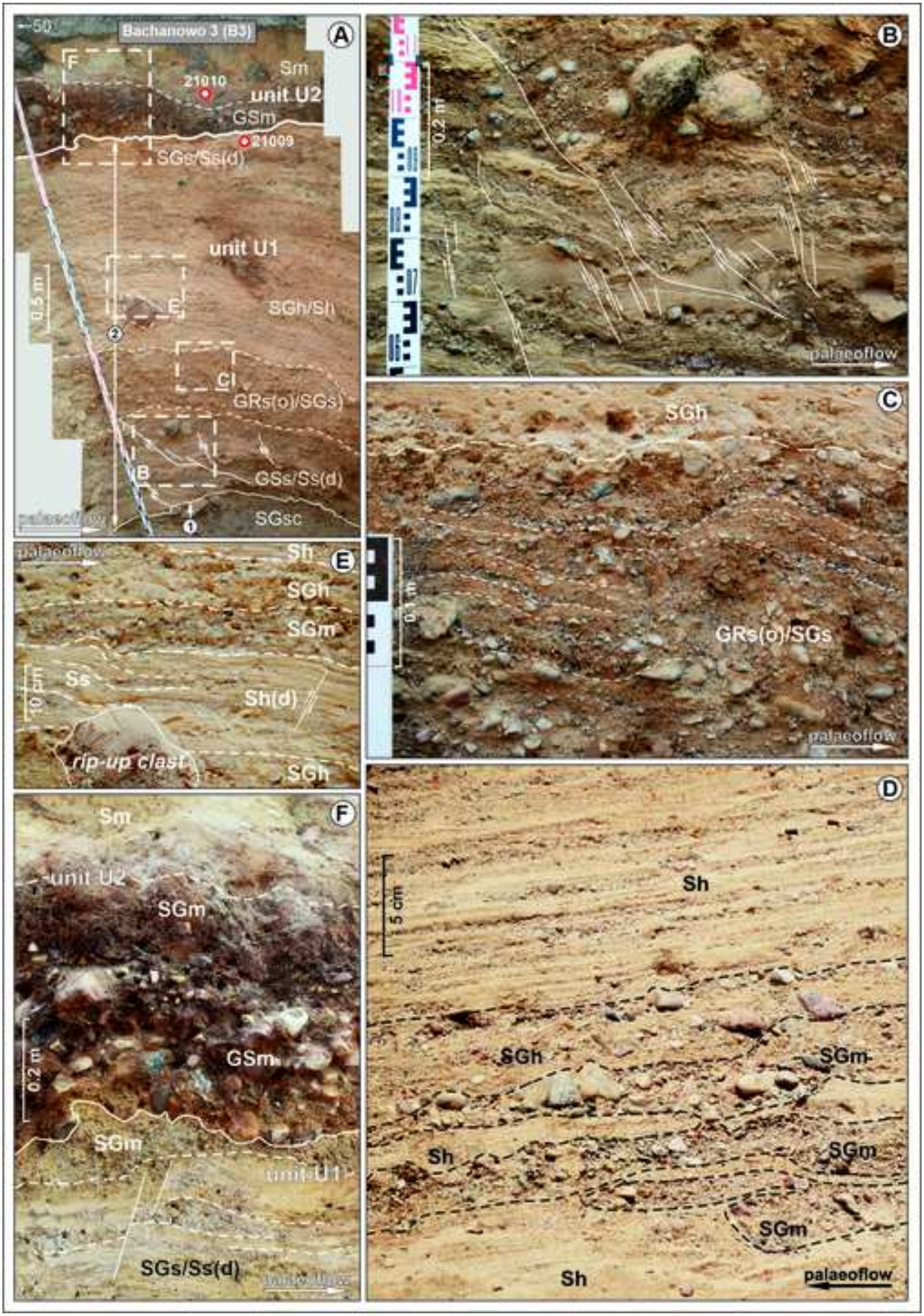

Figure 12 (Color)

Click here to access/download;Figure (Color);Weckwerth et al_Fig_12_corrected.jpg

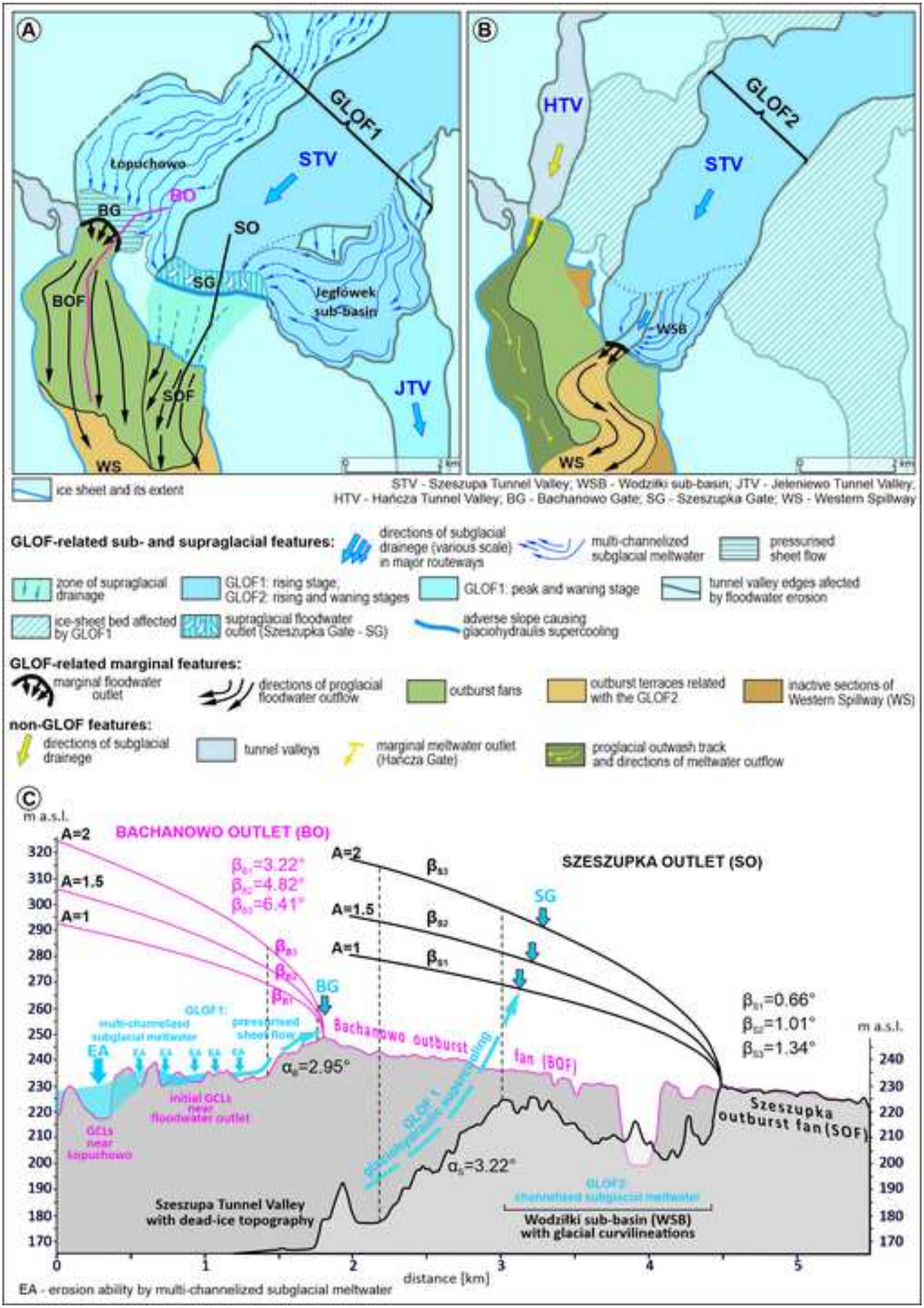

Figure 13 (Color) Click here to access/download;Figure (Color);Weckwerth et al_Fig_13_corrected.jpg

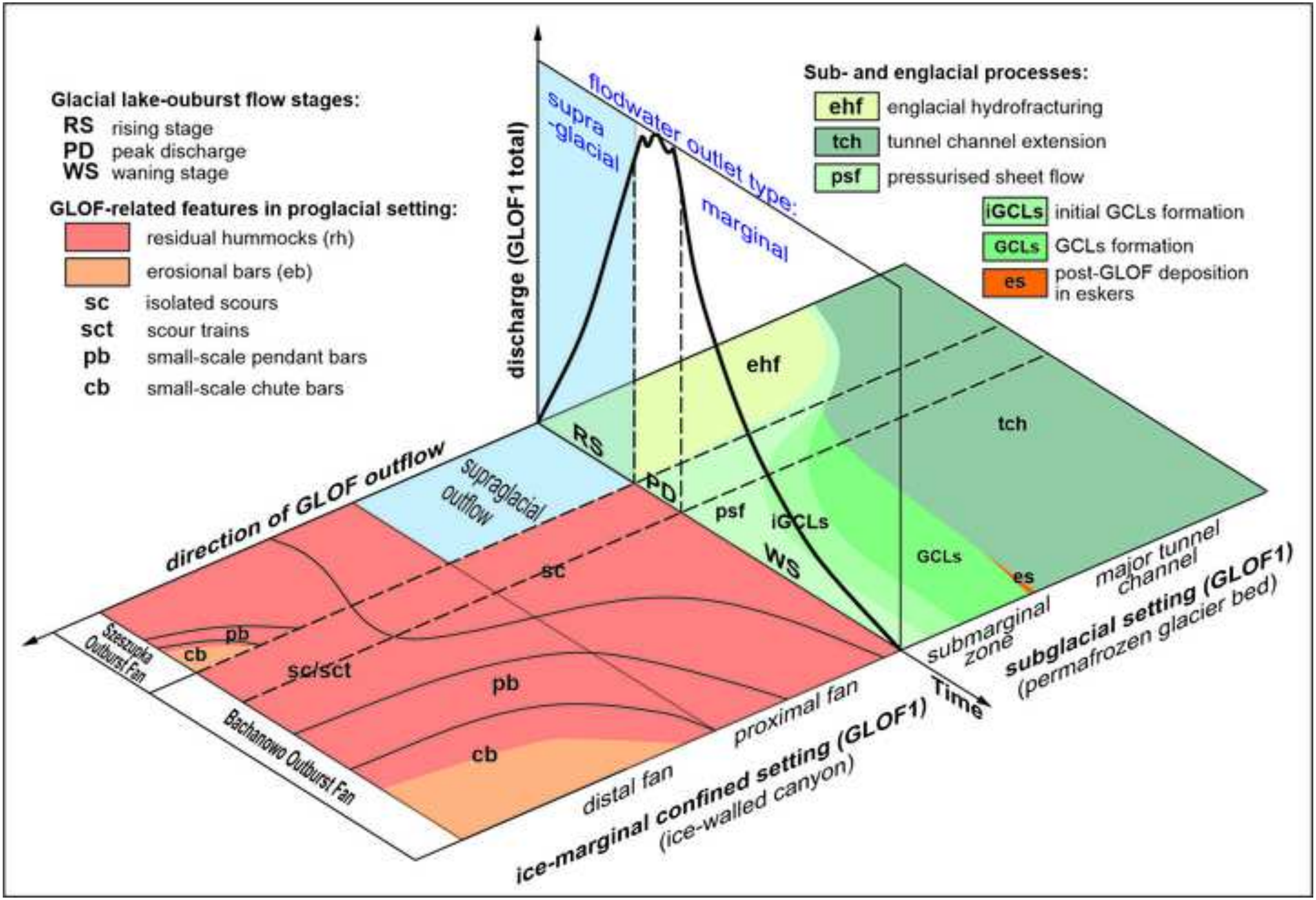

Figure 14 (Color)

Click here to access/download;Figure (Color);Fig_14_new_corrected_Round_2.jpg